

## Statistical data for system-based reliability analysis of stainless steel structures

Itsaso Arrayago<sup>a,\*</sup>, Kim J.R. Rasmussen<sup>b</sup>, Esther Real<sup>a</sup>

<sup>a</sup> *Universitat Politècnica de Catalunya, Dept. of Civil and Environmental Engineering, Spain*

<sup>b</sup> *The University of Sydney, School of Civil Engineering, Australia*

\* Corresponding author: Itsaso Arrayago, Jordi Girona 1-3, Building C1, 08034 Barcelona, Spain, itsaso.arrayago@upc.edu

### ABSTRACT

Current structural codes for steel structures such as AISC 360-10, AS 4100 and Eurocode 3 are based on the traditional member-based *two-step* design approach. However, the most recent versions of these Standards already incorporate preliminary versions of direct or *one-step* system-based design alternatives, which represent a change in the paradigm of structural design. These new direct system-based methods are based on the design-by-analysis concept and allow evaluating the strength of structures directly from numerical simulations. Nevertheless, it is necessary to build a rigorous structural reliability framework to investigate acceptable target reliability indices for structural systems and to provide adequate system safety factors, since these codes do not provide safety factors or reliability requirements for structural systems for design-by-analysis approaches. While this framework has been developed based on advanced Finite Element analysis for hot-rolled and cold-formed carbon steel structures in recent years in the form of the Direct Design Method (DDM), the framework does not exist for stainless steel structures. This paper presents the first step towards developing a system-based reliability framework for stainless steel structures by statistically characterizing the main random parameters affecting the strength of stainless steel structures through a comprehensive database collected from the literature. Based on the collected data, appropriate probabilistic models are proposed for geometric properties, material properties, imperfections and residual stresses of different stainless steel alloys and cross-section or product types. While primarily aimed at providing statistical data for system-based reliability analyses, the data is equally applicable to member-based reliability analyses as described in existing codes.

## KEYWORDS

stainless steel structures; advanced analysis; probability-based design; reliability calibration; structural reliability

## HIGHLIGHTS

- Data on most relevant random variables is collected through a comprehensive literature review.
- Data for different stainless steel alloys and cross-section types are analysed.
- The variability of parameters affecting the strength of stainless steel structures is statistically characterized.
- Appropriate statistical functions and probabilistic models are provided for geometry, material, imperfections and residual stresses.
- Foundational data is provided for the full reliability framework, from which system safety factors and resistance factors can be derived.

## 1. INTRODUCTION

The most commonly accepted approach for determining structural reliability, i.e. the probability of failure of a system of structural members, is to assess the reliability of a structural system by requiring the probability of loads  $Q$  exceeding the structural resistance  $R$  (or reaching a certain limit state) to be less than an adopted target value, in which models for resistance and loading are individually defined. Design of structures is based on traditional limit state criteria following a *two-step* approach where internal actions are first determined from a structural analysis and limit states are subsequently checked for members and connections. Provisions for these checks are given by structural codes for the particular materials, e.g. steel [1-4], in which design parameters and their random variations are modelled by nominal or characteristic values based on partial coefficient methods.

However, the exponential growth of the computational power of standard desktop computers and rapid advances in design software during the past decades have made it possible to accurately predict the behaviour and failure of complex structural systems, providing engineers with the opportunity to progress from the current *two-step* member-based design method to a direct system-based design-by-analysis approach. One of these system-based methods is the Direct Design Method (DDM), which is

based on advanced Finite Element analysis. With the DDM, the strength of structures can be directly evaluated from numerical simulations, eliminating the need for subsequently checking member and connection resistances. The DDM ensures a more uniform reliability of the complete structure across a range of structural systems [5], can be applied equally to simple and complex geometries, and as such encourages innovation, and has the potential to lead to lighter and more economical designs [6-9].

A few structural codes for carbon steel (AS 4100 [3], AISC 360-10 [4]) already incorporate provisions for analysis-based design, but do not provide adequate reliability requirements for structural systems. In this context, a new part of Eurocode 3 is being developed for steel structures, *Part 1-14: Design assisted by finite element analysis* [10], which will include provisions for how to create finite element models to be used in design. Although these Standards require “a comparable or higher level of reliability” than existing member-based provisions be achieved when designing by analysis, they do not include provisions or guidance on acceptable target reliability indices  $\beta$  for structural systems, or do they provide system-based safety factors or give guidance on how to determine these. Thus, determining appropriate system resistance factors  $\phi_s$ , or system safety factors  $\gamma_{Ms}$ , based on rigorous structural reliability considerations is fundamental for the variety of structure types and materials covered by these design codes.

In recent years, design recommendations have been proposed for hot-rolled carbon steel frames [6,7], steel storage rack frames [8], cold-formed steel frames [9] and steel scaffolds [11] in the framework of the Direct Design Method. However, such reliability analysis framework does not exist for stainless steel structures. This will be addressed in the NewGeneSS project [12], which will develop the basis of the DDM design method for stainless steel structures. This paper presents the statistical characterisation of the variability and distribution of the main random parameters affecting the strength of stainless steel structures. The characterisation will serve as mandatory input to the reliability framework from which the system safety factors  $\gamma_{Ms}$  and system resistance factors  $\phi_s$  will be derived. The paper presents a comprehensive database collected from the literature for the most relevant random variables, including geometric properties, material properties, imperfections and residual stresses for

the most common stainless steel cross-section types and alloys, and appropriate statistical functions as well as probabilistic models derived from the data.

## **2. GEOMETRIC PROPERTIES**

### **2.1. CROSS-SECTION DIMENSIONS**

Cross-section dimensions are fundamental variables affecting the strength and stability of stainless steel structures. Current design provisions include design expressions that explicitly depend on magnitudes directly associated with nominal cross-section dimensions, such as cross-section area, second moment of area and section modulus, and are usually provided by manufacturers. However, these nominal dimensions are slightly different from the measured actual dimensions, presenting random variability due to the manufacturing processes, and thus it is necessary to characterize the uncertainty of the random variables defining cross-section geometries.

Fabrication tolerances can be found in different international Standards, including EN 1090-2 [13] AISC 303-10 [14] and AS/NZS 1365 [15], which define maximum deviations allowed from the nominal variables and provide information on the upper boundary of the investigated variabilities. Several research works studying geometric uncertainties on steel structures can be found in the literature, but they mainly focus on hot-rolled [16,17] or cold-formed [9,18] carbon steel profiles. Studies of stainless steel specimens are scarcer and generally limited to the work conducted by Afshan et al. [19] and Lin et al. [20,21] on a relatively small number of specimens. This paper investigates the variability of cross-section dimensions for a wide range of stainless steel product types available based on an extensive database collected from the literature, assuming that measured dimensions reported by international research groups are representative of specimens delivered in practical applications.

The assembled database includes 1070 cold-formed Square and Rectangular Hollow Sections (SHS and RHS) [22-61], 165 cold-formed Circular Hollow Sections (CHS) [29,44,62-71], 204 welded I-sections [45,49,57,64,68,72-77], 27 welded channel sections [78-79], 260 cold-formed channel and lipped channel sections [80-88], 49 hot-rolled angle sections [89-91] and 20 cold-formed angle sections [79,92]. For all section types, the most common austenitic, ferritic, duplex and lean duplex grades were

included (EN 1.4301, 1.4306, 1.4318, 1.4435, 1.4541, 1.4571, 1.4404, 1.4003, 1.4509, 1.4512, 1.4462, 1.4162, 1.4062). The random variables investigated for each cross-section type are defined in Figure 1.

Measured values of the key geometric variables were normalized with respect to the corresponding nominal dimensions and weighted mean, pooled standard deviations and coefficients of variation (COV) were calculated from Eq. 1 and Eq. 2, in order to minimize the effect of the different measurement and data management techniques used by independent authors. In these equations  $n_i$  is the number of measurements in data set  $i$ , while  $\mu_{X,i}$  and  $\sigma_{X,i}$  are the mean value and standard deviation of the random variable  $X$  for data set  $i$ , and  $k$  is the total number of individual datasets considered. The random variable  $X$  is the ratio between a measured dimension and its nominal value.

$$\mu_{X,\text{weighted}} = \frac{\sum_{i=1}^k n_i \mu_{X,i}}{\sum_{i=1}^k n_i} \quad \text{Eq. 1}$$

$$\sigma_{X,\text{pooled}} = \sqrt{\frac{\sum_{i=1}^k (\sigma_{X,i}^2 (n_i - 1))}{\sum_{i=1}^k n_i - k}} \quad \text{Eq. 2}$$

Results are reported in Table 1 for the different stainless steel cross-section types, including the number of specimens used in the determination of the statistics of each random variable, the calculated mean ( $\mu_{X,\text{weighted}}$ ), standard deviation ( $\sigma_{X,\text{pooled}}$ ) and coefficient of variation (COV), and the most suitable statistical distribution fitting the data. The analysis indicated that in general, outer cross-section dimensions (including height, width and diameter) tend to be very close to the nominal values, while measured thicknesses differ more from the nominal values, being slightly lower on average and showing considerably higher variability. All cross-section dimension random variables were found to be approximately normally distributed. Typical histograms corresponding to the investigated cross-section dimensions are shown in Figure 2, representing measured-to-nominal height ratios for SHS/RHS and I-sections and measured-to-nominal thickness ratios for CHS. In general, these results are in line with the variability measurements reported in [19-21] and in prEN 1993-1-1, Annex E [1] for equivalent stainless steel and carbon steel cross-sections, but showing lower variation than the COV value of 0.05 given in [20,21].

Although the corner radius is an important parameter defining square and rectangular hollow sections, nominal values are usually not provided by manufacturers. Recommendations can be found in

the literature and in the recent Design Manual for Stainless Steel Structures [93], which indicate that the internal corner radius  $r_i$  should be taken as  $r_i = 2t$  if no measurements are available, where  $t$  is the section thickness. Since the collected database on SHS and RHS included measurements of the external  $R$  or the internal  $r_i$  corner radius for a large number of specimens, the recommendation of using  $r_i = 2t$  is assessed in this paper. It is important to note that when the corner regions of SHS and RHS specimens are examined, the thickness in these areas is not completely uniform due to the high plastic strains occurring during the forming process. Thus, assuming the external radius is equal to the internal radius plus the thickness can be inaccurate. Consequently, corner radius measurements are analysed separately for the reported external and internal radii, by normalizing data with the nominal thickness and calculating the mean and standard deviations of the measured radius-to-nominal thickness ratios,  $R/t_n$  and  $r_i/t_n$ . The results are reported in Table 1 and indicate very similar dimensions for the corner radius regardless of whether the reference dimension is taken as the external corner radius ( $R = 2t_n$ ) or the internal radius ( $r_i = t_n$ ) for cold-formed SHS and RHS. It is also worth noting that the scatter observed for radii measurements is high, especially for the internal radius, owing to the difficulties associated with taking these measurements.

The variability of the individual random variables defining cross-section dimensions investigated in Table 1 is fundamental for the definition of the numerical simulations for the subsequent structural reliability analyses for direct analysis methods. However, in terms of the statistical validation of proposed design approaches following the traditional *two-stage* member-based approach, the effect of individual parameters on the final geometric variation parameter  $V_{\text{geom}}$  depends on the considered resistance functions  $g_{rt}$  [19]. For the calculation of the geometric coefficients of variation for compression and bending, Eq. 3 and the procedure described in [19] were followed, in which  $w_i$  is the weighting factor of the random variable  $X_i$ , calculated from Eq. 4, while  $V_i$  and  $\mu_i$  correspond to the coefficient of variation and mean value of the random variable  $X_i$ , respectively.

$$V_{\text{geom}}^2 = \sum_{i=1}^n (w_i V_i)^2 \quad \text{Eq. 3}$$

$$w_i = \frac{\frac{\partial g_{rt}}{\partial X_i} \mu_i}{g_{rt}(X_m)} \quad \text{Eq. 4}$$

Results for the geometric variability are reported in Table 2, which show a major influence of the variability of the thickness on the calculated geometric variation parameters for both compression and bending. This follows from the fact that the calculated  $V_{\text{geom}}$  parameters are very similar to the corresponding thickness COV values while the variability of outer cross-section dimension parameters is considerably lower (see Table 1). Results reported in Table 1 and Table 2 are in line with the results reported in [19], although the estimated variabilities of the different variables are lower in this analysis since the collected database was considerably more extensive. Calculated  $V_{\text{geom}}$  values are also comparable to the values reported in the literature for carbon steel sections [16], reporting  $V_A = 0.02$  and  $V_W = 0.02$  values for I-sections in compression and bending, respectively. Note that considerably higher values of geometric variability  $V_{\text{geom}} = 0.05$  were adopted in the development of the AISC stainless steel design guide [94] and in [20].

## 2.2. SPECIMEN LENGTH

The length of specimens also has an important influence on the strength of stainless steel structures and the final layout of structures. To calculate the statistical parameters of the variability of the specimen length, measured lengths of experimental specimens reported in the literature were compared with the corresponding nominal values and weighted mean, pooled standard deviations and coefficients of variation (COV) were calculated. Results are reported in Table 3 for the different cross-section types and for the entire combined database, from which it is concluded that actual specimen lengths are marginally longer than the corresponding nominal values on average, and can be approximated by normal distributions for all sections investigated.

## 3. MATERIAL PROPERTIES

### 3.1. GENERAL

The second main group of random variables governing the strength of structures are material properties. For stainless steels, material parameters are expected to introduce a higher level of uncertainty in structural reliability analysis due to the pronounced nonlinearity of the stress-strain curve, the

significantly large number of alloys available, anisotropy and asymmetry of cross-sections. The material model most commonly used for the description of the nonlinear stress-strain response of stainless steel alloys is the two-stage model developed by Mirambell and Real [95] shown in Eq. 5, which was based on the Ramberg-Osgood model [96,97]. Basic nominal material properties are defined in structural [2,93] and material Standards (EN 10088-1 [98] and EN 10088-4 [99]) for different stainless steel grades.

$$\varepsilon = \begin{cases} \frac{\sigma}{E} + 0.002 \left( \frac{\sigma}{f_y} \right)^n & \text{for } \sigma \leq f_y \\ \frac{\sigma - f_y}{E_{0.2}} + \varepsilon_{0.2} + \left( \varepsilon_u - \varepsilon_{0.2} - \frac{f_u - f_y}{E_{0.2}} \right) \left( \frac{\sigma - f_y}{f_u - f_y} \right)^m & \text{for } \sigma > f_y \end{cases} \quad \text{Eq. 5}$$

In Eq. 5,  $E$  is the Young's modulus,  $f_y$  is the yield stress (usually adopted as the 0.2% proof stress),  $E_{0.2}$  is the tangent modulus at the 0.2% proof stress,  $\varepsilon_{0.2}$  is the total strain at the 0.2% proof stress,  $f_u$  and  $\varepsilon_u$  are the ultimate strength and corresponding total strain, respectively, and  $n$  and  $m$  are the strain hardening exponents. A comprehensive analysis on material modelling of stainless steel alloys was conducted in [100] and expressions for predicting the different parameters involved in Eq. 5 were proposed, but the variability with respect to their nominal values was not investigated. Therefore, it is necessary to statistically define these material parameters to allow their random variations to be modelled in the advanced analysis of stainless steel members and systems. The sensitivity of the system strength to the individual material parameters will be investigated in the future for different types of stainless steel structural systems and failure modes (i.e. yielding and instability modes).

The variability of the material properties of carbon steel structures has been extensively investigated [9,16,17], but only a few studies on the variability of the yield stress  $f_y$  and the ultimate tensile strength  $f_u$  are available for stainless steels [19,20,101]. Table 4 summarizes the overstrength ratios (i.e. measured-to-nominal yield stress and ultimate tensile strength ratios) and respective COV values recommended in the literature over the last decades. The latter are based on extensive databases collected from international manufacturers and additional tests on stainless steel plate and sheet materials. Note that while the overstrength values recommended in [19,101] correspond to the nominal material properties defined in the European EN 10088-4 [99] Standard, values in [20] refer to the

equivalent US ASTM-A666 [102] Standard. However, these studies did not incorporate other fundamental material parameters such as the Young's modulus, strain hardening parameters and the ultimate strain. With the aim of providing information on the variability of these parameters, and with no access to data from manufacturers, an extensive database was collected from the literature including information on austenitic [26,29-32,36,42,44,45,49-52,54,57,58,61,63-66,67,70-79,86-88,90,92,100, 103-117], ferritic [22,25,27,36-38,40,41,55,56,63,80,83,86-88,100,103,104,111,118-122] and duplex/lean-duplex grades [28,33,39,47,48,52,53,55,61,63-65,68,87,100,103,111,123-127]. The database contained data on more than 1400 specimens, covering specimens tested on base material (plates and sheets) and cold-formed material (flat, corner regions of SHS and RHS, and CHS). The investigated base material samples included plate thickness values ranging between 1 mm and 20 mm, while the thickness of the samples extracted from cold-formed specimens varied between 1 mm and 10 mm, with overall cross-section dimensions between 20 mm and 315 mm. This information was used in this paper to define statistical parameters and distributions for the Young's modulus, yield stress, ultimate strength, ultimate strain and strain hardening parameters, which are presented in the following sub-sections.

### 3.2. YOUNG'S MODULUS

Young's modulus or modulus of elasticity  $E$  is the slope of the initial part of the stress-strain curve, and a key parameter defining the deformation of stainless steel structural members and the stiffness of stainless steel structures as well as their strength when failure is governed by instability modes. For typical hot-rolled carbon steel, the slope of the stress-strain curve is constant until the yield point, but for cold-formed carbon steels and stainless steels the slope gradually decreases after the proportionality stress is reached and yielding commences. Current structural and material standards for stainless steel [2,93,98] provide slightly different nominal values for the Young's modulus: while [2,93] adopt a unique value of 200 GPa for the three main stainless steel types, [98] provides a value of 200 GPa for most common austenitic, duplex and lean duplex grades and 220 GPa for ferritic grades.

However, the values of the Young's modulus reported in the literature show considerably different values, as shown in Table 5, where the weighted mean, pooled standard deviations and coefficients of

variation of the Young's modulus are provided separately for plates and sheets and for cold-formed material. The results indicate that the nominal values provided in standards tend to slightly overestimate the Young's modulus, especially for austenitic grades. From Table 5 it can also be appreciated that cold-forming processes have little effect on the value of the Young's modulus, as anticipated in [128], showing similar levels of variability to those observed for plates and for the entire database. Histograms of Young's modulus for different stainless steel types including plate and cold-formed material are shown in Figure 3, which suggest that the adoption of normal distributions is reasonable for the three material types.

### 3.3. YIELD STRESS $f_y$

Characterized by gradual yielding, stainless steels do not present a clearly defined yield stress as for common structural steel, and thus the 0.2% proof stress is conventionally adopted as the equivalent yield stress  $f_y$ . It represents one of the most fundamental parameters in the design of stainless steel structures. Minimum specified yield stress values are defined in the corresponding material Standard EN 10880-4 [99], defined as the characteristic values corresponding to the 95% confidence limit. The same characteristic values are assumed to represent the nominal values according to EN 1990 [129]. Table 6 reports the statistical data for the variability of the yield stress values collated in this paper for plate and sheet specimens. Although the number of data represented only a small proportion of the vast databases analysed in [19] and [101], calculated overstrength ratios and COV values show a good agreement with the values reported in Table 4, especially for the most recent values recommended in [101]. The data analysed also suggest that a log-normal function can be adopted to describe the distribution of the yield stress, which is in line with the recommendations provided by the JCSS [130]. The overstrength ratios provided in [19] have been utilized in the reliability calibrations of several design provisions for the European EN 1993-1-4 Standard, including expressions for both plated structures and cold-formed specimens.

Table 7 shows the variability of the yield stress for cold-formed materials, including the overstrength ratios. The latter demonstrate that the measured-to-nominal ratios are considerably higher and more scattered for the reference nominal yield stress values provided in EN 10880-4 [99], which can be

attributed to the strength enhancements arising from the plastic strains occurring during the cold-forming process. In order to achieve more consistent overstrength ratios for all stainless steel product types, the measured yield stresses were also normalized by the enhanced nominal yield stresses calculated from the predictive enhancement models proposed in [93,128] for cold-formed specimens, which are based on the nominal material and cross-section properties. The results are included in Table 7, in which lower overstrength ratios and coefficients of variation can be observed. Although it is considered that the overstrength ratios based on extensive databases for plate and sheet material properties can be conservatively adopted for cold-formed materials, by assuming that the higher scatter will be compensated by the considerably higher overstrength ratios, the recommendation, when a more accurate characterization of the variability of the yield stress is required, is to adopt the reference enhanced yield stress based on nominal properties in conjunction with overstrength ratios and COV values equal to 1.30, 1.30, 1.15 and 0.15, 0.15, 0.15 for cold-formed austenitic, ferritic and duplex stainless steels, respectively. Figure 4 shows the histograms for the overstrength ratios for the yield stress for the cold-formed stainless steel families, referred to as the enhanced nominal yield stress values, fitted by log-normal distributions. Results for plate and sheet materials also showed that the most suitable statistical distribution was a log-normal distribution.

### 3.4. ULTIMATE TENSILE STRENGTH $f_u$

The ultimate tensile strength  $f_u$  corresponds to the maximum stress value of the stress-strain curve prior to failure. Although less significant than the yield stress because it is generally not a design variable for structural members, it provides an indirect measurement of the level of strain hardening characterizing stainless steels. Following the same procedure as for the yield stress, measured ultimate strength  $f_u$  values from the assembled database were compared with the corresponding nominal values given in EN 10088-4 [99] for each grade. As for yield stress, the nominal (minimum) ultimate strength  $f_{u,nom}$  is the characteristic value corresponding to the 95% confidence limit. Statistical data on the variability of the ultimate strength is presented in Table 8 for different stainless steel types investigated in this paper, with results for the different product types reported separately. According to the results published in [19], the overstrength factors for the ultimate strength  $f_{u,mean}/f_{u,nom}$  ranged between 1.06 and 1.23 for

plate and sheet materials, with no clear correlation with the associated COV. Although the databases utilized for the recommendations in [19,101] were considerably more extensive than the sample population analysed in this paper, results show that the calculated overstrength ratios for plate and sheet materials are in line with those reported in Table 4. Results also suggest that cold-formed materials present considerably more scattered overstrength ratios than plates and sheets, showing higher overstrength ratios for austenitic stainless steel alloys, but similar values for ferritic and duplex grades. From these results, it is recommended that the same overstrength factor provided for plates and sheets also be adopted for cold-formed materials, and the associated COV value be increased to 0.10 to account for the more scattered results. The data was accurately fitted by log-normal distributions in all cases, as shown in Figure 5 for cold-formed stainless steel materials.

### 3.5. ULTIMATE STRAIN $\epsilon_u$

The ultimate strain  $\epsilon_u$  is one of the material parameters most affected by the plastic deformations occurring during forming processes, decreasing considerably when compared to the corresponding base sheet or plate material values [100]. Statistical parameters of the ultimate strain for plates and sheets and cold-formed material are reported separately in Table 9 for austenitic, ferritic and duplex stainless steel alloys. These results highlight the reduction observed in the ultimate strain for cold-formed coupons and indicate that austenitic stainless steels show the highest deformation capacity, followed by duplex and ferritic grades. The results also indicate that the data can be accurately fitted by normal distributions.

### 3.6. STRAIN HARDENING PARAMETERS $n$ AND $m$

The roundness of the nonlinear stress-strain curve is controlled by the strain hardening exponent  $n$  for the low strain range, and by the strain hardening exponent  $m$  for the high strain range, being key parameters in the material definition of stainless steel alloys. These parameters cannot be directly measured from experimental stress-strain curves; rather they need to be optimized or estimated through numerical techniques. The strain hardening exponent values considered in this paper were optimized following the procedure described in [119] for those stress-strain curves acquired as raw data, whereas the values reported in the literature were otherwise assumed.

Table 10 summarizes the weighted mean, pooled standard deviations and coefficients of variation for the strain hardening parameter  $n$ . Results are provided separately for different stainless steel and product types, since alloying elements and cold-working tend to considerably influence the parameter [100]. The data for the strain hardening parameter  $n$  was fitted with log-normal distributions, as shown in the histograms presented in Figure 6 for different cold-formed stainless steel types. From the statistical results reported in Table 10, it can be concluded that the cold-working process induces a slightly more rounded stress-strain response, providing lower  $n$  values for cold-formed specimens than for plates and sheets. This is more relevant for ferritic grades, which show the highest  $n$  values. Note that the mean values reported in Table 10 for plates and sheets are slightly higher than the nominal values provided in [2,93], while values for cold-formed material are lower than the nominal values. This is because these nominal values were based on the analysis conducted in [100], in which, for simplicity, no distinction was made between product type in the proposed  $n$  values. Similar results are presented in Table 11 for the strain hardening parameter  $m$ , in which the effect of the cold-forming is also evident for all stainless steel types. However, higher values were observed for cold-formed specimens in this case, due to the reduction of the ultimate strain and the slight increase in ultimate strength occurring during the cold-forming process, which cause the increase in the strain hardening parameter  $m$  observed from the data. Although more scattered, log-normal distributions were also observed to adequately fit the collected data.

#### **4. INITIAL GEOMETRIC IMPERFECTIONS**

Random variables related to initial geometric imperfections represent the third fundamental source of uncertainty to be considered in the analysis and design of stainless steel structures. Their effect is to introduce additional load eccentricities and increase second order effects, causing the premature failure of the structure. Initial geometric imperfections inevitably occur in stainless steel structures despite the strict manufacturing and installation tolerance requirements, and thus imperfections need to be explicitly introduced in finite element models, or implicitly incorporated through the analytical resistance functions provided in national codes for the current *two-step* member-based design approach. For the calibration of the direct design methods assisted by finite element analysis, imperfections need

to be included and treated as random variables to account for these uncertainties in the reliability studies. Statistics corresponding to local cross-sectional, member and global frame imperfections are analysed in the following sub-sections for stainless steel structures.

#### 4.1. LOCAL IMPERFECTIONS

Local cross-section imperfections are defined as deviations of the different plate elements composing the cross-section from the perfect geometry, and include distortional-shaped and local-shaped modes. For cold-formed hollow sections (SHS, RHS and CHS) the latter are more relevant since the transverse stiffness of hollow sections is considerably high, whereas for open sections (including I-sections and channels) both types can be important.

The amplitude of local imperfections  $w_{0,local}$  in carbon steel sections has traditionally been estimated by means of different predictive models, the simplest of which define the local imperfection amplitude as a fraction of the wall thickness [9,130], while deviation tolerances given in EN 1090-2 [13] are expressed as fractions  $\gamma_1$  of plate width  $b$  ( $\pm b/\gamma_1$ ), with  $\gamma_1 = 100$  for welded sections and  $\gamma_1 = 50$  for cold-formed sections. However, the adoption of the local imperfection factor as a fraction of the plate thickness or width was found to be unsuitable as a general parameter for cold-formed sections, and the alternative model given by Eq. 6 was developed by Dawson and Walker [131] for simply supported plates in carbon steel, with  $\gamma_2 = 0.2$ . In this equation  $f_y$  is the yield stress (or the 0.2% proof stress) and  $\sigma_{cr}$  corresponds to the plate critical buckling stress. This model was adapted to stainless steel SHS and RHS sections by Gardner and Nethercot [132], where the coefficient  $\gamma_2 = 0.023$  was proposed. Despite being initially based upon just 15 imperfection measurements, it has been subsequently been found to be adequate by independent researchers.

$$\frac{w_{0,local}}{t} = \gamma_2 \frac{f_y}{\sigma_{cr}} \quad \text{Eq. 6}$$

Since no study is available in the literature for local imperfections on stainless steel cross-sections, despite the considerable database of reported local imperfection measurements available in the literature, this paper presents a comprehensive analysis of local imperfection amplitudes for different cross-section shapes. The collected database includes measurements for cold-formed SHS and RHS sections [22-27,32,33,37,39,47,48,52,54-56,132], welded I-sections [73-76], welded channel sections

[78-79], cold-formed channel and lipped channel sections [87], hot-rolled angle sections [89-91] and cold formed angle sections [92], including specimens made from different stainless steel types. The analysis is presented separately for welded and cold-formed sections. Results corresponding to the calculated  $\gamma_1$  factors for welded I-sections, channels and angles are reported in Table 12, where the different geometric properties  $B_n$  and  $H_n$  correspond to those defined in Figure 1 for each section type. The  $\gamma_1$  factors were found to follow a normal distribution for I-sections and a log-normal distribution for angle sections. On the contrary, the data available for channel sections did not allow determining an appropriate statistical distribution and thus only the mean and standard deviation values are reported in this paper.

The data on local imperfection amplitudes for cold-formed stainless steel sections is plotted in Figure 7, where it is compared with the original predictive model (Eq. 6 with  $\gamma_2 = 0.023$ ). The results show that data on SHS and RHS can be grouped in two sets, named Group 1 and Group 2, showing considerably different imperfection amplitudes. While data for Group 1 is similar to the imperfection measurements reported for angle and channel sections, lying close to the original proposal (Eq. 6 with  $\gamma_2 = 0.023$ ), Group 2 exhibits considerably larger imperfections. This difference can be explained by specimens being supplied by different stainless steel manufacturers with different quality control requirements, and by the adoption of different procedures for the measurement of imperfection amplitudes. A review of the data indicated that most specimens were delivered by the same manufacturer, but results for each data Group corresponded to different measurement techniques: while results included in Group 1 [22-27,32,47,48,54-56,132] were acquired from longitudinal measurements at the different faces comprising SHS and RHS members, measurements in Group 2 [33,37,39,52] were obtained through perimetral (transversal) readings at different cross-sections along the member. In this paper, the results are treated independently for the two Groups. Regression fits for SHS/RHS Group 2 and data for other sections can be observed in Figure 7. It can be noticed that while the regression fit for Group 1, with  $\gamma_2 = 0.024$ , is very similar to the original proposal [132], the factor for Group 2 is considerably higher,  $\gamma_2 = 0.094$ . In view of these results, and for simplicity, it is recommended that the original factor  $\gamma_2 = 0.023$  is adopted for the prediction of local imperfection amplitudes of cold-formed

sections when no measurement is available in deterministic analyses. Statistical information on the  $\gamma_2$  parameter for the different cold-formed cross-sections is provided in Table 13. For both groups, the data was found to follow log-normal distributions.

## 4.2. MEMBER IMPERFECTIONS

Member imperfections are bow-shaped deviations from the perfect geometry in which cross-sections are displaced or rotate as whole, and are generally associated with global buckling shapes. These initial member imperfections have a considerable effect on member capacity as they increase second order effects and can cause premature failure. They are implicitly considered in the resistance functions provided in current standards [1-4], such as through the adoption of buckling curves for the flexural buckling resistance of columns. However, for the reliability studies required for the derivation of system safety factors these inevitable imperfections need to be explicitly characterized and included in the finite element simulations.

Member imperfections have been extensively investigated for hot-rolled and cold-formed steel members [9,16,130] and are traditionally represented by a half sine-wave with a maximum amplitude given by a fraction of the member length  $L$ ,  $w_{0,member} = L/K$ . Despite the considerable database available from international research groups reporting measured imperfection values from experimental specimens during the last decades, to the authors' knowledge no equivalent studies can be found in the literature for stainless steel columns. Thus, reported bow imperfection amplitudes at the member mid-length section, where the maximum deviation is most likely to appear, were collected from the literature on austenitic, ferritic, duplex and lean duplex stainless steel members with different cross-section types, and the analysis is presented in this section. Weighted mean, pooled standard deviations and coefficients of variation corresponding to the mid-length member imperfection amplitude are reported in Table 14 in terms of the length fraction  $K$ , while histograms for SHS/RHS, CHS and I-sections are shown in Figure 8. According to the results reported in Table 14, the measured member imperfections tend to be considerably lower than the corresponding tolerances stipulated in EN 1090-2 [13] (i.e.  $L/750$ ) and imperfection values adopted in the development of the buckling curves in European Standards [1,2] (i.e.  $L/1000$ ). Values are also considerably lower on average than those regularly adopted in numerical

simulations [32,47,56,63] (i.e.  $L/1000$ ,  $L/1500$ ), but it should be noted that initial geometric imperfections are sometimes used to indirectly incorporate the combined effect of different types of imperfections in numerical simulations, such as residual stresses. Results in Figure 8 also indicate that the data on member imperfection amplitudes can be reasonably fitted by log-normal distributions for the different cross-section types investigated.

However, assuming member imperfections as half sine-waves (represented by the first buckling mode) in conjunction with the mid-length amplitude value does not provide information about the contribution of higher buckling modes showing multiple waves [133]. Following the procedure described in [133], initial member geometric imperfections were assumed to be a linear combination of a given number of modes  $n$ , with individual buckling modes being sine-shaped with different amplitude factors as per Eq. 7. In this equation  $a_i$  is the scale factor for the  $i^{\text{th}}$  mode and  $x$  is the non-dimensional coordinate along the length of the member.

$$w_{0,\text{member}} = \sum_{i=1}^n L \cdot a_i \sin(i\pi x) \quad \text{Eq. 7}$$

To treat member imperfections as random variables defined by random shapes and magnitudes, detailed measurements along the member are required, which are not commonly measured nor reported in the literature. Thus, the database on continuous measurements of member imperfections assembled in this paper is more limited, including data on SHS and RHS [25,26,109], CHS [68] and lipped channel [86] sections. Based on these data, initial member imperfections were modelled as linear combinations of the first three buckling modes ( $n = 3$  in Eq. 7), from which scale factors were determined by solving a system of equations for each member. Mean scale factors were then determined to match the mean imperfection amplitudes reported in Table 14, which represented a larger sample of mid-length measurements, and taking into account that only the first and the third modes contribute to the imperfection in this section, as described in [133]. Table 15 presents the statistical information about the obtained scale factors for the different cross-section types investigated. According to the results, the first buckling mode governs the member imperfections of the cross-section shapes investigated and should be sufficient for an accurate approximation of initial imperfections, with  $a_1$  amplitudes equivalent to  $L/3333$ ,  $L/3845$  and  $L/5882$  for SHS/RHS, CHS and channel sections, respectively. Scale

factors for the first buckling modes  $a_1$  were found to follow log-normal distributions, similarly to the results shown in Table 14 and Figure 8, while the distributions of  $a_2$  and  $a_3$  were approximately normal.

### 4.3. FRAME IMPERFECTIONS

Frame imperfections are deviations of the overall structure from the perfect geometry, the most representative of which are sway-shaped imperfections. These sway imperfections are usually defined by an out-of-plumb angle and have considerable influence on the strength of structures as they increase second order effects. Maximum column inclination deviations of portal frames according to the erection tolerances given in EN 1090-2 [13] are  $\phi = \pm 1/500$ , although designers often define more strict tolerances for serviceability and operational reasons. Owing to the importance of these imperfections, they need to be incorporated in frame analyses as initial imperfections or equivalent horizontal loads, as per prEN 1993-1-1 [1], with the out-of-plumb angle calculated from a basic angle of  $\phi_0 = \pm 1/200$  and correction factors for height and number of columns in a row.

Contrary to the other imperfection types investigated in this paper, measurements on stainless steel frame imperfections are very scarce. Arrayago et al. [26] recently conducted an experimental programme on stainless steel frames, in which four single-bay single-storey frames made from RHS austenitic stainless steel were tested under static vertical and horizontal loads. Initial imperfections were obtained prior to testing by means of a precision theodolite, measuring the position of several points in each column and along the rafters. In-plane imperfections as well as out-of-plane imperfections were measured. The statistics of the recorded out-of-plumb angles are reported in Table 16. According to [26], two of the frames showed imperfection patterns following sway modes, while the initial geometries of the remaining two frames showed non-sway modes. Note that no statistical distribution is provided in this case, since the data available was too limited.

To characterize frame imperfection uncertainties adequately it is thus necessary to refer to the measurements conducted on carbon steel frames, as discussed in [9], which are also considerably limited. Based on the measurements of initial frame imperfections on general steel structures found in [134,135], a normal out-of-plumb angle distribution with a zero mean and a standard deviation of  $1/610$  was proposed. It is believed that the distributions provided for frame imperfection amplitudes in cold-

formed carbon steel represent an upper bound for stainless steel frames, since workshops for stainless steel structures are generally more specialized and therefore final structures will typically present imperfections with lower amplitude and level of uncertainty.

## **5. RESIDUAL STRESSES**

Residual stresses are stresses that exist in structural sections in their unloaded state, which are primarily generated during the fabrication processes and caused by either differential cooling of different part of the cross-section (in hot-rolled and welded sections) or non-uniform plastic deformations (in cold-formed sections). They are particularly relevant in frames prone to instability failure modes, as they can cause premature yielding and buckling, thus reducing the ultimate strength. Owing to different material and thermal properties, the residual stresses are different in equivalent stainless steel and carbon steel sections and thus need to be independently characterized. Over the last few decades a number of experimental studies have been carried out with the aim of developing residual stress models for different stainless steel section types and fabrication processes, including cold-formed SHS and RHS sections [33,52,136-139], press-braked and hot-rolled angle sections [136,137], welded I-sections [75-77,140] and welded SHS and RHS sections [140], among others.

The residual stress pattern and magnitude vary significantly for different cross-section types, fabrication procedures and material grades, and hence different predictive models can be found in the literature for cold-formed and welded RHS, as well as for austenitic and duplex welded RHS. Consequently, the residual stress data available in the literature were sorted in different sets and only those showing a statistically representative number of specimens were included in the analysis. For the characterization of the uncertainties associated with residual stresses in stainless steel members, a similar approach to that adopted in [141] was followed. In this approach, the residual stress pattern was assumed to be deterministic for each cross-section and fabrication type, while the magnitudes of the residual stresses were considered random variables. For the different measurements available in the literature, appropriate residual stress patterns were fitted to experimental residual stresses by applying a random scale factor. These scale factors corresponding to each specimen  $j$  were calculated according to the method described in [141], which can be summarized as follows: (i) nondimensionalise measured

residual stresses by the corresponding yield stress  $\sigma_{\text{exp},i}/f_y$ ; (ii) calculate the theoretical nondimensionalised residual stress for the considered model at the same points  $\sigma_{\text{model},i}/f_y$ ; (iii) calculate scale factors  $Y_j$  by minimising the total error between the scaled theoretical model and the experimental measurement, as per Eq. 8.

$$\text{Error}_j = \sum_{i=1}^n \left( Y_j \frac{\sigma_{\text{model},i}}{f_y} - \frac{\sigma_{\text{exp},i}}{f_y} \right)^2 \quad \text{Eq. 8}$$

The reference residual stress patterns considered in this study are the models proposed by Gardner and Cruise [137] for cold-formed SHS and RHS and press-braked angle sections, and the models developed by Yuan et al. [140] for welded I-sections and SHS and RHS sections, as summarized in Table 17. Note that some of the residual stress measurements from the literature review provided at the beginning of this section have not been considered in the analysis, since the number of available data was deemed insufficient for an adequate statistical characterization. The statistical data of the derived scale factors are presented in Table 17, while the corresponding histograms are shown in Figure 9. Normal distributions were fitted to the histograms.

## 6. CONCLUSIONS

System-based design approaches represent a change in the paradigm of structural design with a strong potential not only for the design of lighter and more efficient new structures, but also for the reassessment and reinforcement of existing structures. Provisions for analysing by design have been incorporated in several international design codes for steel structures [3,4], but no specific reliability requirements or acceptable target reliability indices are provided for structural systems. In recent years, through the development of the Direct Design Method (DDM), system safety factors and design recommendations have been proposed for different types of steel structures, including hot-rolled and cold-formed frames as well as rack and scaffolding structures. However, the Method has not yet been extended to stainless steel structures, and there is no developed system reliability framework for this material.

For the purpose of providing appropriate system safety factors or resistance factors for finite element-based design approaches for stainless steel structures, this paper presents a comprehensive study of the main random variables influencing the strength of stainless steel structures, including

geometric properties, material parameters, imperfections and residual stresses. Based on an extensive database collected from the literature, statistical functions and probabilistic models are provided for different random variables affecting the behaviour and strength of stainless steel cold-formed and welded cross-sections (including square and rectangular hollow sections, circular hollow sections, I-sections, channels and angles) and the most common austenitic, ferritic, duplex and lean-duplex stainless steel alloys. The collection of geometric properties (section height, width, thickness, corner radius and member length), material parameters (Young's modulus, yield stress, ultimate tensile strength, ultimate strain and strain hardening exponents), imperfections (at local cross-section, member and frame levels) and residual stresses was analysed statistically and appropriate statistical distributions were derived.

The information presented in this paper is fundamental for the development of the full reliability framework for stainless steel structures, including consideration of loads and load combinations for the ultimate and serviceability limit states for different types of stainless steel structural systems and different failure modes. Through Monte-Carlo type simulation procedures, extensive finite element simulations are currently being carried out to determine system strength distributions from which system resistance and safety factors will be proposed for stainless steel structures.

## **ACKNOWLEDGEMENTS**

This research project has received funding from the European Union's Horizon 2020 Research and Innovation Programme under the Marie Skłodowska-Curie Grant Agreement No. 842395. The time dedicated by numerous authors of referenced papers to provide additional data and information is also much appreciated.

## **REFERENCES**

- [1] European Committee for Standardization (CEN). prEN 1993-1-1. Eurocode 3: Design of Steel Structures – Part 1-1: General Rules and Rules for Buildings. Final Document; 2019.
- [2] European Committee for Standardization (CEN). EN 1993-1-4:2006+A1:2015. Eurocode 3: Design of Steel Structures – Part 1-4: General Rules. Supplementary Rules for Stainless Steels, including amendment A1 (2015). Brussels, Belgium, 2015.
- [3] Standards Australia (AS). AS 4100. Steel Structures. Sydney, Australia, 2016.

- [4] American Institute of Steel Construction (ANSI/AISC). AISC 360-10. Specification for Structural Steel Buildings. Illinois, USA, 2016.
- [5] Zhang H., Liu H., Ellingwood B.R. and Rasmussen K.J.R. System reliabilities of planar gravity steel frames designed by the inelastic method in AISC 360-10. *Journal of Structural Engineering (ASCE)* 144(3):04018011, 2018.
- [6] Zhang H., Shayan S., Rasmussen K.J.R. and Ellingwood B.R. System-based design of planar steel frames, I: Reliability framework. *Journal of Constructional Steel Research* 123, 135–143, 2016.
- [7] Zhang H., Shayan S., Rasmussen K.J.R. and Ellingwood B.R. System-based design of planar steel frames, II: Reliability results and design recommendations. *Journal of Constructional Steel Research* 123, 154–161, 2016.
- [8] Sena Cardoso F., Rasmussen K.J.R. and Zhang H. System reliability-based criteria for the design of steel storage rack frames by advanced analysis: Part I – Statistical characterisation of system strength. *Thin-Walled Structures* 141, 713–724, 2019.
- [9] Sena Cardoso F., Zhang H., Rasmussen K.J.R. and Yan S. Reliability calibrations for the design of cold-formed steel portal frames by advanced analysis. *Engineering Structures* 182, 164–171, 2019.
- [10] European Committee for Standardization (CEN). prEN 1993-1-14. Eurocode 3: Design of steel structures – Part 1-14: Design assisted by finite element analysis. Brussels, Belgium. *Under development*.
- [11] Wang C., Zhang H., Rasmussen K.J.R., Reynolds J. and Yan S. Reliability-based limit state design of support scaffolding systems. *Engineering Structures (in press)*, 2020.
- [12] NewGeneSS, New Generation Design Methods for Stainless Steel Structures. Marie Skłodowska-Curie Fellowship 2018, funded by the European Union’s Horizon 2020 Research and Innovation Programme under Grant Agreement No. 842395.
- [13] European Committee for Standardization (CEN). EN 1090-2:2018. Execution of steel structures and aluminium structures. Technical requirements for steel structures. Brussels, Belgium, 2018.
- [14] American Institute of Steel Construction (ANSI/AISC). AISC 303-10. Code of Standard Practice for Steel Buildings and Bridges. Illinois, USA, 2010.
- [15] Australian/New Zealand Standards (AS/NZS). AS/NZS 1365:1996 Tolerances for flat-rolled steel products. NSW, Australia and Wellington, New Zealand, 1996.
- [16] Rang T.N., Galambos T.V. and Yu W.W. Load and resistance factor design of cold-formed steel - Statistical analysis of mechanical properties and thickness of materials combined with calibrations of the AISI design provisions on unstiffened compression elements and connections. Structural Series, University of Missouri-Rolla, Rolla, Missouri, 1979.
- [17] Byfield M.P. and Nethercot D.A. An analysis of the true bending strength of steel beams. *Proceedings of the Institution of Civil Engineers: Structures and Buildings* 128, 188–197, 1988.
- [18] Foley C. Statistics on the thickness of cold-formed hollow sections. Report to AISC 2011.

- [19] Afshan S., Francis P., Baddoo N.R. and Gardner L. Reliability analysis of structural stainless steel design provisions. *Journal of Constructional Steel Research* 114, 293–304, 2015.
- [20] Lin S.-H., Yu W.-W and Galambos T.V. Load and resistance factor design of cold-formed stainless steel statistical analysis of material properties and development of the LRFD provisions. Center for Cold-Formed Steel Structures Library. 72, University of Missouri-Rolla, Missouri, U.S.A., 1988.
- [21] Lin S.-H., Yu W.-W and Galambos T.V. ASCE LRFD Method for Stainless Steel Structures. *Proceedings of the 10<sup>th</sup> International Specialty Conference on Cold-Formed Steel Structures*. Missouri, U.S.A., 1990.
- [22] Afshan S. and Gardner L. Experimental Study of Cold-Formed Ferritic Stainless Steel Hollow Sections. *Journal of Structural Engineering (ASCE)* 139, 717–728, 2013.
- [23] Arrayago I. and Real E. Experimental Study on Ferritic Stainless Steel RHS and SHS Cross-sectional Resistance Under Combined Loading. *Structures* 4, 69–79, 2015.
- [24] Arrayago I. and Real E. Experimental study on ferritic stainless steel simply supported and continuous beams. *Journal of Constructional Steel Research* 119, 50–62, 2016.
- [25] Arrayago I., Real E. and Mirambell E. Experimental study on ferritic stainless steel RHS and SHS beam-columns. *Thin-Walled Structures* 100, 93–104, 2016.
- [26] Arrayago I., González de León I., Real E. and Mirambell E. Tests on stainless steel frames. Part I: preliminary tests and experimental setup. Submitted to *Thin-Walled Structures*, 2020.
- [27] Bock M., Arrayago I. and Real E. Experiments on cold-formed ferritic stainless steel slender sections. *Journal of Constructional Steel Research* 109, 13–23, 2015.
- [28] Cai Y. and Young B. Web crippling of lean duplex stainless steel tubular sections under concentrated end bearing loads. *Thin-Walled Structures* 134, 29–39, 2019.
- [29] Feng R., Liu Y. and Zhu J. Tests of CHS-to-SHS tubular connections in stainless steel. *Engineering Structures* 199, 109590, 2019.
- [30] Gardner L. and Nethercot D.A. Experiments on stainless steel hollow sections – Part 1: Material and cross-sectional behaviour. *Journal of Constructional Steel Research* 60, 1291–1318, 2004.
- [31] Gardner L. and Nethercot D.A. Experiments on stainless steel hollow sections – Part 2: Member behaviour of columns and beams. *Journal of Constructional Steel Research* 60, 1319–1332, 2004.
- [32] Gardner L., Talja A. and Baddoo N.R. Structural design of high-strength austenitic stainless steel. *Thin-Walled Structures* 44, 517–528, 2006.
- [33] Huang Y. and Young B. Material properties of cold-formed lean duplex stainless steel sections. *Thin-Walled Structures* 54, 72–81, 2012.
- [34] Huang Y. and Young B. Tests of pin-ended cold-formed lean duplex stainless steel columns. *Journal of Constructional Steel Research* 82, 203–215, 2013.
- [35] Huang Y. and Young B. Experimental investigation of cold-formed lean duplex stainless steel beam-columns. *Thin-Walled Structures* 76, 105–117, 2014.

- [36] Hyttinen V. Design of cold-formed stainless steel SHS beam-columns. Report 41, University of Oulu, Oulu, Finland, 1994.
- [37] Islam S.M.Z. and Young B. Ferritic stainless steel tubular members strengthened with high modulus CFRP plate subjected to web crippling. *Journal of Constructional Steel Research* 77, 107–118, 2012.
- [38] Islam S.M.Z. and Young B. Strengthening of ferritic stainless steel tubular structural members using FRP subjected to Two-Flange-Loading. *Thin-Walled Structures* 62, 179–190, 2013.
- [39] Islam S.M.Z. and Young B. FRP strengthening of lean duplex stainless steel hollow sections subjected to web crippling. *Thin-Walled Structures* 85, 183–200, 2014.
- [40] Li H.T. and Young B. Cold-formed ferritic stainless steel tubular structural members subjected to concentrated bearing loads. *Engineering Structures* 145, 392–405, 2017.
- [41] Li H.T. and Young B. Web crippling of cold-formed ferritic stainless steel square and rectangular hollow sections. *Engineering Structures* 176, 968–980, 2018.
- [42] Liu Y. and Young B. Buckling of stainless steel square hollow section compression members. *Journal of Constructional Steel Research* 59, 165–177, 2003.
- [43] Lui W.M., Ashraf M. and Young B. Tests of cold-formed duplex stainless steel SHS beam-columns. *Engineering Structures* 74, 111–121, 2014.
- [44] Rasmussen K.J.R. and Hancock G.J. Design of Cold-Formed Stainless Steel Tubular Members. I: Columns. *Journal of Structural Engineering* 119(8), 2349–2367, 1993.
- [45] Real E. and Mirambell E. Flexural behaviour of stainless steel beams. *Engineering Structures* 27, 1465–1475, 2005.
- [46] Talja A. and Salmi P. Design of Stainless Steel RHS Beams, Columns and Beam Columns. Research Note 1619, VTT Building Technology, Finland, 1995.
- [47] Theofanous M. and Gardner L. Testing and numerical modelling of lean duplex stainless steel hollow section columns. *Engineering Structures* 31, 3047–3058, 2009.
- [48] Theofanous M. and Gardner L. Experimental and numerical studies of lean duplex stainless steel beams. *Journal of Constructional Steel Research* 66, 816–825, 2010.
- [49] Theofanous M., Saliba N., Zhao O. and Gardner L. Ultimate response of stainless steel continuous beams. *Thin-Walled Structures* 83, 115–127, 2014.
- [50] VTT. WP 3 Members with Class 4 cross-sections in fire. Technical Report, VTT Building Technology, Finland, 2007.
- [51] Young B. and Liu Y. Experimental Investigation of Cold-Formed Stainless Steel Columns. *Journal of Structural Engineering (ASCE)* 129, 169–176, 2003.
- [52] Young B. and Lui W.M. Behavior of Cold-Formed High Strength Stainless Steel Sections. *Journal of Structural Engineering (ASCE)* 131(11), 1738–1745, 2005.
- [53] Young B. and Lui W.M. Tests of cold-formed high strength stainless steel compression members. *Thin-Walled Structures* 44, 224–234, 2006.

- [54] Zhao O., Rossi B., Gardner L. and Young B. Behaviour of structural stainless steel cross-sections under combined loading – Part I: Experimental study. *Engineering Structures* 89, 236–246, 2015.
- [55] Zhao O., Rossi B., Gardner L. and Young B. Experimental and Numerical Studies of Ferritic Stainless Steel Tubular Cross Sections under Combined Compression and Bending. *Journal of Structural Engineering (ASCE)*, 04015110-2, 2015.
- [56] Zhao O., Gardner L. and Young B. Buckling of ferritic stainless steel members under combined axial compression and bending. *Journal of Constructional Steel Research* 117, 35–48, 2016.
- [57] Zheng B., Hua X. and Shu G. Tests of cold-formed and welded stainless steel beam-columns. *Journal of Constructional Steel Research* 111, 1–10, 2015.
- [58] Zhou F. and Young B. Tests of cold-formed stainless steel tubular flexural members. *Thin-Walled Structures* 43, 1325–1337, 2005.
- [59] Zhou F. and Young B. Design and tests of cold-formed stainless steel sections subjected to concentrated bearing load. *Advances in Steel Structures* 1, 487–496, 2005.
- [60] Zhou F. and Young B. Cold-Formed Stainless Steel Sections Subjected to Web Crippling. *Journal of Structural Engineering (ASCE)* 132(1), 134–144, 2006.
- [61] Zhou F. and Young B. Experimental and numerical investigations of cold-formed stainless steel tubular sections subjected to concentrated bearing load. *Journal of Constructional Steel Research* 63, 1452–1466, 2007.
- [62] Bardi F.C. and Kyriakides S. Plastic buckling of circular tubes under axial compression – Part I: Experiments. *International Journal of Mechanical Sciences* 48 830–841, 2006.
- [63] Buchanan C., Real E. and Gardner L. Testing, simulation and design of cold-formed stainless steel CHS columns. *Thin-Walled Structures* 130, 297–312, 2018.
- [64] Burgan B.A., Baddoo N.R. and Gilsean K.A. Structural design of stainless steel members – comparison between Eurocode 3, Part 1.4 and test results. *Journal of Constructional Steel Research* 54, 51–73, 2000.
- [65] He A. and Zhao O. Experimental and numerical investigations of concrete-filled stainless steel tube stub columns under axial partial compression. *Journal of Constructional Steel Research* 158, 405–416, 2019.
- [66] Kiyamaz G. Strength and stability criteria for thin-walled stainless steel circular hollow section members under bending. *Thin-Walled Structures* 43, 1534–1549, 2005.
- [67] Rasmussen K.J.R. and Hancock J.G. Design of Cold-Formed Stainless Steel Tubular Members. II: Beams. *Journal of Structural Engineering* 119(8), 2368–2386, 1993.
- [68] Talja A. Test report on welded I and CHS beams, columns and beam-columns. Research Report for WP3. VTT Building Technology, Finland, 1997.
- [69] Young B. and Hartono W. Compression Tests of Stainless Steel Tubular Members. *Journal of Structural Engineering (ASCE)* 128,754–761, 2002.

- [70] Zhao O., Gardner L. and Young B. Structural performance of stainless steel circular hollow sections under combined axial load and bending – Part1: Experiments and numerical modelling. *Thin-Walled Structures* 101, 231–239, 2016.
- [71] Zhao O., Gardner L. and Young B. Testing and numerical modelling of austenitic stainless steel CHS beam–columns. *Engineering Structures* 111, 263–274, 2016.
- [72] Bu Y. and Gardner L. Laser-welded stainless steel I-section beam-columns: Testing, simulation and Design. *Engineering Structures* 179, 23–36, 2019.
- [73] dos Santos, G.B. and Gardner L. Testing and numerical analysis of stainless steel I-sections under concentrated end-one-flange loading. *Journal of Constructional Steel Research* 157, 271–281, 2019.
- [74] dos Santos, G.B., Gardner L. and Kucuckler M. Experimental and numerical study of stainless steel I-sections under concentrated internal one-flange and internal two-flange loading. *Engineering Structures* 175, 355–370, 2018.
- [75] Gardner L., Bu Y. and Theofanous M. Laser-welded stainless steel I-sections: Residual stress measurements and column buckling tests. *Engineering Structures* 127, 536–548, 2016.
- [76] Sun Y. and Zhao O. Material response and local stability of high-chromium stainless steel welded I-sections. *Engineering Structures* 178, 212–226, 2019.
- [77] Wang Y., Yang L., Gao B., Shi Y. and Yuan H. Experimental Study of Lateral-torsional Buckling Behavior of Stainless Steel Welded I-section Beams. *International Journal of Steel Structures* 14(2), 411–420, 2014.
- [78] Liang Y., Zhao O., Long Y.L. and Gardner L. Stainless steel channel sections under combined compression and minor axis bending – Part 1: Experimental study and numerical modelling. *Journal of Constructional Steel Research* 152, 154–161, 2019.
- [79] Theofanous M., Liew A. and Gardner L. Experimental study of stainless steel angles and channels in bending. *Structures* 4, 80–90, 2015.
- [80] Yousefi A.M., Lim J.B.P. and Clifton G.C. Web bearing capacity of unlipped cold-formed ferritic stainless steel channels with perforated web subject to end-two-flange (ETF) loading. *Engineering Structures* 152, 804–818, 2017.
- [81] Yousefi A.M., Lim J.B.P. and Clifton G.C. Cold-formed ferritic stainless steel unlipped channels with web openings subjected to web crippling under interior-two-flange loading condition – Part I: Tests and finite element model validation. *Thin-Walled Structures* 116, 333–341, 2017.
- [82] Yousefi A.M., Lim J.B.P. and Clifton G.C. Web Crippling Behavior of Unlipped Cold-Formed Ferritic Stainless Steel Channels Subject to One-Flange Loadings. *Journal of Structural Engineering (ASCE)* 144(8), 04018105, 2018.
- [83] Yousefi A.M., Lim J.B.P. and Clifton G.C. Cold-formed ferritic stainless steel unlipped channels with web perforations subject to web crippling under one-flange loadings. *Construction and Building Materials* 191, 713–725, 2018.

- [84] Yousefi A.M., Lim J.B.P. and Clifton G.C. Web crippling strength of perforated cold-formed ferritic stainless steel unlipped channels with restrained flanges under one-flange loadings. *Thin-Walled Structures* 137, 94–105, 2019.
- [85] Yousefi A.M., Lim J.B.P. and Clifton G.C. Web crippling design of cold-formed ferritic stainless steel unlipped channels with fastened flanges under end-two-flange loading condition. *Journal of Constructional Steel Research* 152, 12–28, 2019.
- [86] Becque J. and Rasmussen K.J.R. Experimental investigation of local-overall interaction buckling of stainless steel lipped channel columns. *Journal of Constructional Steel Research* 65, 1677–1684, 2009.
- [87] Lecce M. and Rasmussen K.J.R. Distortional Buckling of Cold-Formed Stainless Steel Sections: Experimental Investigation. *Journal of Structural Engineering (ASCE)* 132(4), 497–504, 2006.
- [88] Niu S., Rasmussen K.J.R. and Fan F. Distortional–global interaction buckling of stainless steel C-beams: Part I — Experimental investigation. *Journal of Constructional Steel Research* 96, 127–139, 2014.
- [89] Liang Y., Jeyapragasam V.V.K., Zhang L. and Zhao O. Flexural-torsional buckling behaviour of fixed-ended hot-rolled austenitic stainless steel equal-leg angle section columns. *Journal of Constructional Steel Research* 154, 43–54, 2019.
- [90] de Menezes A.A., da S. Vellasco P.C.G., de Lima L.R.O., da Silva A.T. Experimental and numerical investigation of austenitic stainless steel hot-rolled angles under compression. *Journal of Constructional Steel Research* 152, 42–56, 2019.
- [91] Sun Y., Liu Z., Liang Y. and Zhao O. Experimental and numerical investigations of hot-rolled austenitic stainless steel equal-leg angle sections. *Thin-Walled Structures* 144, 106225, 2019.
- [92] Zhang L., Tan K.H. and Zhao O. Experimental and numerical studies of fixed-ended cold-formed stainless steel equal-leg angle section columns. *Engineering Structures* 184, 134–144, 2019.
- [93] Steel Construction Institute (SCI). Design Manual for Structural Stainless Steel. Fourth Edition, 2017.
- [94] AISC, Design Guide 27: Structural Stainless Steel, American Institute of Steel Construction, 2013.
- [95] Mirambell E. and Real E. On the calculation of deflections in structural stainless steel beams: an experimental and numerical investigation. *Journal of Constructional Steel Research* 54(4), 109-133, 2000.
- [96] Ramberg W. and Osgood W.R. Description of stress-strain curves by three parameters. Technical Note No. 902. Washington, D.C., USA. National Advisory Committee for Aeronautics, 1943.
- [97] Hill H.N. Determination of stress-strain relations from "offset" yield strength values. Technical Note No. 927, 1944.
- [98] European Committee for Standardization (CEN). EN 10088-1. Stainless Steels Part 1: List of stainless steels. Brussels, Belgium, 2005.

- [99] European Committee for Standardization (CEN). EN 10088-4. Stainless Steels Part 4: Technical Delivery Conditions for Sheet/Plate and Strip of Corrosion Resisting Steels for Construction Purposes. Brussels, Belgium, 2009.
- [100] Arrayago I., Real E. and Gardner L. Description of stress–strain curves for stainless steel alloys. *Materials and Design* 87, 540–552, 2015.
- [101] Steel Construction Institute (SCI). Proposed material factors for EN 1993-1-4. Technical Report. UK, 2020.
- [102] American Society for Testing, and Materials (ASTM). Standard Specification for Austenitic Stainless Steel, Sheet, Strip, Plate, and Flat Bar for Structural Applications. ASTM Designation: ASTM A666-84, 1984.
- [103] Afshan S., Rossi B. and Gardner L. Strength enhancements in cold-formed structural sections – Part I: Material testing. *Journal of Constructional Steel Research* 83, 177–188, 2013.
- [104] Becque J., Rasmussen K.J.R. Experimental investigation of the interaction of local and overall buckling of stainless steel I-columns. *Journal of Structural Engineering (ASCE)* 135(11), 1340–1348, 2009.
- [105] Elflah M., Theofanous M., Dirar S., Yuan H. Behaviour of stainless steel beam-to-column joints – Part 1: Experimental investigation. *Journal of Constructional Steel Research* 152, 183–193, 2019.
- [106] Real E., Mirambell E. and Estrada I. Shear response of stainless steel plate girders. *Engineering Structures* 29, 1626–1640, 2007.
- [107] Fan S., Liu F., Zheng B., Shu G. and Tao Y. Experimental study on bearing capacity of stainless steel lipped C section stub columns. *Thin-Walled Structures* 83, 70–84, 2014.
- [108] Han L.H., Chen F., Liao F.Y., Tao Z. and Uy B. Fire performance of concrete filled stainless steel tubular columns. *Engineering Structures* 56, 165–181, 2013.
- [109] Ning K., Yang L., Yuan H. and Zhao M. Flexural buckling behaviour and design of welded stainless steel box-section beam-columns. *Journal of Constructional Steel Research* 161, 47–56, 2019.
- [110] Nip K.H., Gardner L. and Elghazouli A.Y. Cyclic testing and numerical modelling of carbon steel and stainless steel tubular bracing members. *Engineering Structures* 32(2), 424–441, 2010.
- [111] Rasmussen K.J.R. Full-range stress–strain curves for stainless steel alloys, Research Report No. R811, Department of Civil Engineering. The University of Sydney, 2001.
- [112] Rasmussen K.J.R. and A.S. Hasham A.S. Tests of X- and K-joints in CHS stainless steel tubes. *Journal of Structural Engineering (ASCE)* 127(10), 1183–1189, 2001.
- [113] Rasmussen K.J.R. and Young B. Tests of X- and K-joints in SHS stainless steel tubes. *Journal of Structural Engineering (ASCE)* 127(10), 1173–1182, 2001.
- [114] Uy B., Tao Z. and Han L.H. Behaviour of short and slender concrete-filled stainless steel tubular columns. *Journal of Constructional Steel Research* 67, 360–378, 2011.

- [115] Xu M. and Szalyga M. Comparative Investigations on the Load-bearing Behaviour of Single Lap Joints with Bolts Stressed in Shear and Bearing-experimental and Simulation. Master Project at the University of Duisburg-Essen, Institute for Metal and Lightweight Structures, 2011.
- [116] Young B. and Hartono W. Compression Tests of Stainless Steel Tubular Members. *Journal of Structural Engineering (ASCE)* 128,754–761, 2002.
- [117] Yousuf M., Uy B., Tao Z., Remennikov A. and Liew J.Y.R. Transverse impact resistance of hollow and concrete filled stainless steel columns. *Journal of Constructional Steel Research* 82, 177–189, 2013.
- [118] Manninen T. Technical report for Structural applications of ferritic stainless steels (SAFSS). WP1 end-user requirements and material performance. Task 1.3 Characterization of stress– strain behaviour: Technical Specifications for Room-Temperature: Tensile and Compression Testing, 2011.
- [119] Real E., Arrayago I., Mirambell E. and Westeel R. Comparative study of analytical expressions for the modelling of stainless steel behaviour. *Thin-Walled Structures* 83 2–11, 2014.
- [120] Rossi B. Mechanical behaviour of ferritic grade 3Cr12 stainless steel. Part 1: Experimental investigations. *Thin-Walled Structures* 48, 553–560, 2010.
- [121] Talja A. and Hradil P. Structural performance of steel members: model calibration tests. Research report for SAFSS-WP2. Internal Report, VTT Building Technology, Finland, 2011.
- [122] Tondini N., Rossi B., Franssen J.M. Experimental investigation on ferritic stainless steel columns in fire. *Fire Safety Journal* 62, 238–248, 2013.
- [123] Ellobody E. and Young B. Structural performance of cold-formed high strength stainless steel columns. *Journal of Constructional Steel Research* 61, 1631–1649, 2005.
- [124] Rasmussen K.J.R., Burns T., Bezkorovainy P., Bambach M.R. Numerical modelling of stainless steel plates in compression. *Journal of Constructional Steel Research* 59, 1345–1362, 2003.
- [125] Saliba N. and Gardner L. Experimental study of the shear response of lean duplex stainless steel plate girders. *Engineering Structures* 46, 375–391, 2013.
- [126] Saliba N. and Gardner L. Cross-section stability of lean duplex stainless steel welded I-sections. *Journal of Constructional Steel Research* 80, 1–14, 2013.
- [127] Young B. and Ellobody E. Experimental investigation of concrete-filled cold-formed high strength stainless steel tube columns. *Journal of Constructional Steel Research* 62, 484–492, 2006.
- [128] Rossi B., Afshan S. and Gardner L. Strength enhancements in cold-formed structural sections – Part II: Predictive models. *Journal of Constructional Steel Research* 83, 189–196, 2013.
- [129] European Committee for Standardization. EN 1990. European Committee for Standardization Eurocode. Basis of structural design. Brussels, Belgium, 2005.
- [130] Joint Committee on Structural Safety (JCSS). Probabilistic Model Code, Zurich, Switzerland, 2001.
- [131] Dawson R.G. and Walker A.C. Post-buckling of geometrically imperfect plates. *Journal of the Structural Division (ASCE)* 98(1), 75–94, 1972.

- [132] Gardner L. and Nethercot D.A. Numerical modelling of stainless steel structural components - A consistent approach. *Journal of Structural Engineering (ASCE)* 130(10), 1586–1601, 2004.
- [133] Shayan S., Rasmussen K.J.R. and Zhang Hao. On the modelling of initial geometric imperfections of steel frames in advanced analysis. *Journal of Constructional Steel Research* 98, 167–177, 2014.
- [134] Beaulieu D. and Adams P.F. The results of a survey on structural out-of-plumbs. *Canadian Journal of Civil Engineering* 5(4), 462–70, 1978.
- [135] Lindner J. and Gietzelt R. Assumptions for imperfections for out-of-plumb of columns. *Stahlbau* 53, 97–102, 1984.
- [136] Cruise R.B. and Gardner L. Residual stress analysis of structural stainless steel sections. *Journal of Constructional Steel Research* 64 352–366, 2008.
- [137] Gardner L. and Cruise R.B. Modeling of Residual Stresses in Structural Stainless Steel Sections. *Journal of Structural Engineering (ASCE)* 135(1), 42–53, 2009.
- [138] Jandera M., Gardner L. and Machacek J. Residual stresses in cold-rolled stainless steel hollow sections. *Journal of Constructional Steel Research* 64, 1255–1263, 2008.
- [139] Zheng B., Shu G. and Jiang Q. Experimental study on residual stresses in cold rolled austenitic stainless steel hollow sections. *Journal of Constructional Steel Research* 152, 94–104, 2019.
- [140] Yuan H.X., Wang Y.Q., Shi Y.J. and Gardner L. Residual stress distributions in welded stainless steel sections. *Thin-Walled Structures* 79, 38–51, 2014.
- [141] Shayan S., Rasmussen K.J.R. and Zhang, H. Probabilistic modelling of residual stress in advanced analysis of steel structures. *Journal of Constructional Steel Research* 101, 407–414, 2014.

## TABLES

Table 1. Cross-sectional dimension variations for different stainless steel section types.

Cross-section type	Random variable	No. specimens	Mean	Std. Dev.	COV	Statistical distribution	References
SHS/RHS	Height, H	1070	$1.002 \cdot H_n$	$0.012 \cdot H_n$	0.012	Normal	[22-61]
	Width, B	1070	$1.002 \cdot B_n$	$0.010 \cdot B_n$	0.010	Normal	
	Thickness, t	1058	$0.974 \cdot t_n$	$0.028 \cdot t_n$	0.029	Normal	
	Int. Radius, R	842	$1.030 \cdot t_n$	$0.317 \cdot t_n$	0.308	-	
	Ext. Radius, R	181	$2.180 \cdot t_n$	$0.307 \cdot t_n$	0.141	-	
CHS	Diameter, D	165	$0.999 \cdot D_n$	$0.003 \cdot D_n$	0.003	Normal	[29,44,62-71]
	Thickness, t	162	$0.982 \cdot t_n$	$0.035 \cdot t_n$	0.035	Normal	
I-sections	Height, H	204	$0.998 \cdot H_n$	$0.007 \cdot H_n$	0.007	Normal	[45,49,57,64,68,72-77]
	Width, B	204	$1.001 \cdot B_n$	$0.007 \cdot B_n$	0.007	Normal	
	Web thickness, $t_w$	165	$0.999 \cdot t_n$	$0.027 \cdot t_n$	0.027	Normal	
	Flange thickness, $t_f$	172	$1.000 \cdot t_n$	$0.031 \cdot t_n$	0.031	Normal	
Channels – Welded	Height, H	27	$1.003 \cdot H_n$	$0.003 \cdot H_n$	0.003	Normal	[78-79]
	Width, B	27	$0.995 \cdot B_n$	$0.005 \cdot B_n$	0.005	Normal	
	Thickness, t	27	$0.975 \cdot t_n$	$0.033 \cdot t_n$	0.034	Normal	
Channels – Cold-formed	Height, H	260	$1.008 \cdot H_n$	$0.003 \cdot H_n$	0.003	Normal	[80-88]
	Width, B	260	$1.001 \cdot B_n$	$0.004 \cdot B_n$	0.004	Normal	
	Lip, C	80	$0.988 \cdot C_n$	$0.018 \cdot C_n$	0.018	Normal	
	Thickness, t	260	$0.965 \cdot t_n$	$0.026 \cdot t_n$	0.027	Normal	
Angles – Hot-rolled	Leg, B	49	$0.998 \cdot B_n$	$0.008 \cdot B_n$	0.008	Normal	[89-91]
	Thickness, t	49	$0.977 \cdot t_n$	$0.027 \cdot t_n$	0.028	Normal	
Angles – Cold-formed	Leg, B	20	$1.000 \cdot B_n$	$0.004 \cdot B_n$	0.004	Normal	[79,92]
	Thickness, t	20	$0.988 \cdot t_n$	$0.021 \cdot t_n$	0.021	Normal	

Note: the subscript  $n$  represents the nominal value.

Table 2. Calculated values for the COV of geometric properties for stainless steel sections in compression and bending.

Cross-section type	No. specimens	$V_{geom}$ compression	$V_{geom}$ bending
SHS and RHS	1058	0.029	0.027
CHS	162	0.035	0.035
I-sections	165	0.019	0.025
Channels – Cold-formed	260	0.042	0.043
Channels – Welded	27	0.023	0.023
Angles	69	0.018	0.018

Table 3. Member length L variations for different stainless steel section types.

Cross-section type	No. specimens	Mean	Std. Dev.	COV	Statistical distribution	References
SHS/RHS	969	1.001	0.004	0.004	Normal	[22-61]
CHS	127	1.000	0.001	0.001	Normal	[29,44,62-71]
I-sections	172	1.006	0.006	0.006	Normal	[45,49,57,64,68,72-77]
Channels – Cold-formed	228	1.000	0.001	0.001	Normal	[78-79]
Channels – Welded	15	1.000	0.002	0.002	Normal	[80-88]
Angles	69	0.998	0.004	0.004	Normal	[79,89-92]
All	1580	1.001	0.051	0.051	Normal	-

Table 4. Yield stress  $f_y$  and ultimate strength  $f_u$  variation proposals in the literature.

Variable	Stainless steel type	Mean	COV	Reference
Yield stress $f_y$	Austenitic and Ferritic	1.10 <sup>1</sup>	0.100	[20]
	Austenitic	1.30 <sup>2</sup>	0.060	[19]
	Ferritic	1.20 <sup>2</sup>	0.045	
	Duplex	1.10 <sup>2</sup>	0.030	
	Austenitic	1.20 <sup>2</sup>	0.059	[101]
	Ferritic	1.15 <sup>2</sup>	0.056	
	Duplex	1.10 <sup>2</sup>	0.054	
Ultimate strength $f_u$	Austenitic and Ferritic	1.10 <sup>1</sup>	0.050	[20]
	All	1.10 <sup>2</sup>	0.035	[19]
	All	1.10 <sup>2</sup>	0.025	[101]

<sup>1</sup>: overstrength ratios correspond to nominal values in ASTM A666-84 [102].

<sup>2</sup>: overstrength ratios correspond to nominal values in EN 10088-4 [99].

Table 5. Young's modulus E variations for different stainless steel and product types.

Stainless steel type	Product type	No. specimens	Mean [MPa]	Std. Dev. [MPa]	COV	Statistical distribution
Austenitic	Plates & Sheets	299	195416	11175	0.057	Normal
	Cold-formed	497	193084	11039	0.057	
	All	796	193960	11141	0.057	
Ferritic	Plates & Sheets	93	203738	14764	0.072	Normal
	Cold-formed	193	198572	15582	0.078	
	All	286	200252	15486	0.077	
Duplex and Lean Duplex	Plates & Sheets	164	206233	11957	0.058	Normal
	Cold-formed	128	205025	8700	0.042	
	All	292	205703	10653	0.052	

Table 6. Yield stress  $f_y$  variations for different stainless steel plates and sheet materials.

Stainless steel type	No. specimens	Mean	Std. Dev.	COV	Statistical distribution
Austenitic	306	$1.22 \cdot f_{y,n}$	$0.075 \cdot f_{y,n}$	0.061	Log-normal
Ferritic	72	$1.22 \cdot f_{y,n}$	$0.063 \cdot f_{y,n}$	0.052	Log-normal
Duplex and Lean Duplex	83	$1.11 \cdot f_{y,n}$	$0.097 \cdot f_{y,n}$	0.088	Log-normal

Note: the subscript  $n$  represents the nominal value in EN 10088-4 [99].

Table 7. Yield stress  $f_y$  variations for different stainless steel cold-formed materials.

Stainless steel type	Reference yield stress	No. specimens	Mean	Std. Dev.	COV	Statistical distribution
Austenitic	Nominal	363	$1.78 \cdot f_{y,n}$	$0.353 \cdot f_{y,n}$	0.199	Log-normal
	Enhanced nominal		$1.39 \cdot f_{y,enh_n}$	$0.220 \cdot f_{y,enh_n}$	0.158	Log-normal
Ferritic	Nominal	175	$1.60 \cdot f_{y,n}$	$0.257 \cdot f_{y,n}$	0.161	Log-normal
	Enhanced nominal		$1.38 \cdot f_{y,enh_n}$	$0.163 \cdot f_{y,enh_n}$	0.118	Log-normal
Duplex and Lean Duplex	Nominal	122	$1.18 \cdot f_{y,n}$	$0.166 \cdot f_{y,n}$	0.140	Log-normal
	Enhanced nominal		$1.16 \cdot f_{y,enh_n}$	$0.140 \cdot f_{y,enh_n}$	0.121	Log-normal

Note: the subscripts  $n$  and  $enh_n$  represent the nominal value in EN 10088-4 [99] and the enhanced nominal values from [93,128], respectively.

Table 8. Ultimate strength  $f_u$  variations for different stainless steel and product types.

Stainless steel type	Product type	No. specimens	Mean	Std. Dev.	COV	Statistical distribution
Austenitic	Plates & Sheets	219	$1.15 \cdot f_{u,n}$	$0.040 \cdot f_{u,n}$	0.034	Log-normal
	Cold-formed	274	$1.33 \cdot f_{u,n}$	$0.124 \cdot f_{u,n}$	0.094	Log-normal
Ferritic	Plates & Sheets	100	$1.12 \cdot f_{u,n}$	$0.099 \cdot f_{u,n}$	0.088	Log-normal
	Cold-formed	155	$1.16 \cdot f_{u,n}$	$0.130 \cdot f_{u,n}$	0.112	Log-normal
Duplex and Lean Duplex	Plates & Sheets	41	$1.10 \cdot f_{u,n}$	$0.026 \cdot f_{u,n}$	0.023	Log-normal
	Cold-formed	86	$1.17 \cdot f_{u,n}$	$0.123 \cdot f_{u,n}$	0.105	Log-normal

Note: the subscript  $n$  represents the nominal value in EN 10088-4 [99].

Table 9. Ultimate strain  $\epsilon_u$  variations for different stainless steel and product types.

Stainless steel type	Product type	No. specimens	Mean [mm/mm]	Std. Dev. [mm/mm]	COV	Statistical distribution
Austenitic	Plates & Sheets	47	0.49	0.06	0.118	Normal
	Cold-formed	102	0.39	0.15	0.373	Normal
Ferritic	Plates & Sheets	98	0.17	0.05	0.280	Normal
	Cold-formed	159	0.13	0.11	0.852	Normal
Duplex and Lean Duplex	Plates & Sheets	85	0.29	0.05	0.171	Normal
	Cold-formed	99	0.24	0.14	0.579	Normal

Table 10. Strain hardening parameter  $n$  variations for different stainless steel and product types.

Stainless steel type	Product type	No. specimens	Mean [-]	Std. Dev. [-]	COV	Statistical distribution
Austenitic	Plates & Sheets	50	10.6	1.8	0.168	Log-normal
	Cold-formed	284	6.0	2.1	0.342	Log-normal
Ferritic	Plates & Sheets	89	16.3	4.9	0.302	Log-normal
	Cold-formed	188	10.1	5.4	0.536	Log-normal
Duplex and Lean Duplex	Plates & Sheets	162	6.6	2.4	0.364	Log-normal
	Cold-formed	120	6.3	2.1	0.332	Log-normal

Table 11. Strain hardening parameter  $m$  variations for different stainless steel and product types.

Stainless steel type	Product type	No. specimens	Mean [-]	Std. Dev. [-]	COV	Statistical distribution
Austenitic	Plates & Sheets	47	2.3	0.3	0.144	Log-normal
	Cold-formed	96	3.1	1.3	0.426	Log-normal
Ferritic	Plates & Sheets	95	2.9	0.3	0.104	Log-normal
	Cold-formed	55	3.5	2.2	0.619	Log-normal
Duplex and Lean Duplex	Plates & Sheets	31	3.6	0.5	0.138	Log-normal
	Cold-formed	33	4.2	1.9	0.462	Log-normal

Table 12. Local imperfection amplitude variations  $\gamma_1$  for different stainless steel welded section types.

Cross-section type	No. specimens	Mean	Std. Dev.	COV	Statistical distribution	References
I-sections	59	$0.0012 \cdot B_n$	$0.0013 \cdot B_n$	1.041	Normal	[73-76]
Channels	27	$0.007 \cdot H_n$	$0.0038 \cdot H_n$	0.541	-	[78-79]
Angles	40	$0.018 \cdot B_n$	$0.0009 \cdot B_n$	0.515	Log-normal	[89-91]

Table 13. Local imperfection amplitude variations  $\gamma_2$  for different stainless steel cold-formed section types.

Cross-section type	No. specimens	Mean	Std. Dev.	COV	Statistical distribution	References
SHS and RHS – Group 1	160	0.041	0.026	0.636	Log-normal	[22-27,32,47,48,54-56,132]
SHS and RHS – Group 2	104	0.117	0.057	0.484	Log-normal	[33,37,39,52]
Channels	16	0.036	0.030	0.828	Log-normal	[87]
Angles	16	0.055	0.064	1.161	Log-normal	[92]

Table 14. Midspan member imperfection amplitude variations for different stainless steel section types.

Cross-section type	No. specimens	Mean	Std. Dev.	COV	Statistical distribution	References
SHS and RHS	226	L/3232	L/5369	0.602	Log-normal	[22,25,26,31,34-36,42-44,47,51,52,56,57]
CHS	55	L/3484	L/6056	0.575	Log-normal	[44,63,68,69,71]
I-sections	43	L/4038	L/7013	0.576	Log-normal	[57,72,75,77]
Channels	29	L/5879	L/12016	0.489	Log-normal	[86]
Angles	16	L/4784	L/25348	0.189	Log-normal	[89]

Table 15. Member imperfection scale factor variations for different stainless steel section types.

Cross-section type	No. specimens	Scale factor	Mean	Std. Dev.	Statistical distribution	References
SHS and RHS	20	a <sub>1</sub>	0.000300·L	0.00026·L	Log-normal	[25,26,109]
		a <sub>2</sub>	0.000005·L	0.00014·L	Normal	
		a <sub>3</sub>	-0.000010·L	0.00011·L	Normal	
CHS	10	a <sub>1</sub>	0.00026·L	0.00016·L	Log-normal	[68]
		a <sub>2</sub>	-0.00001·L	0.00008·L	Normal	
		a <sub>3</sub>	-0.00003·L	0.00009·L	Normal	
Channels	60	a <sub>1</sub>	0.00017·L	0.00017·L	Log-normal	[86]
		a <sub>2</sub>	-0.00001·L	0.00006·L	Normal	
		a <sub>3</sub>	0.00001·L	0.00004·L	Normal	

Table 16. Out-of-plumb angle variations for stainless steel frame imperfections [26].

Direction	No. specimens	Mean	Std. Dev.
In-plane	4	1/672	1/656
Out-of-plane	4	1/159	1/531

Table 17. Variations of residual stress magnitude scale factors for different stainless steel section types.

Cross-section type and fabrication	Stainless steel type	RS model	No. specimens	Mean	Std. Dev.	COV	Statistical distribution	References
Cold-formed SHS and RHS	Austenitic	[137]	13	0.875	0.161	0.184	Normal	[136,138,139]
Press-braked angles	Austenitic	[137]	8	0.284	0.166	0.585	Normal	[136]
Welded I-sections	Austenitic and Duplex	[140]	14	0.819	0.119	0.145	Normal	[77,140]
Welded SHS and RHS	Austenitic and Duplex	[140]	8	0.615	0.115	0.186	Normal	[140]

**FIGURES**

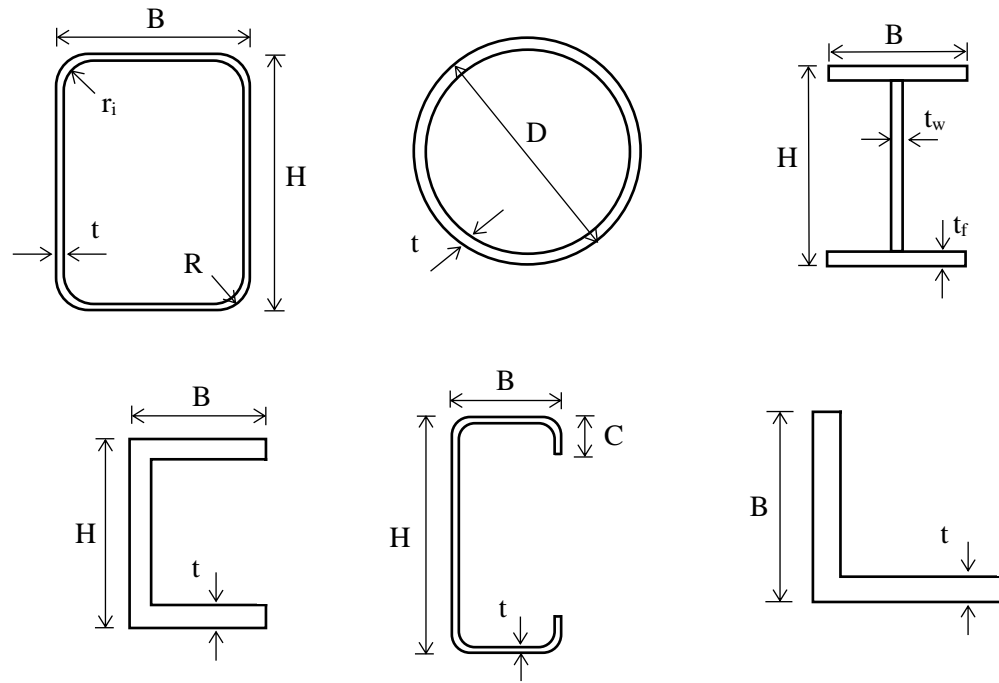


Figure 1. Variables on cross-section properties for different section types.

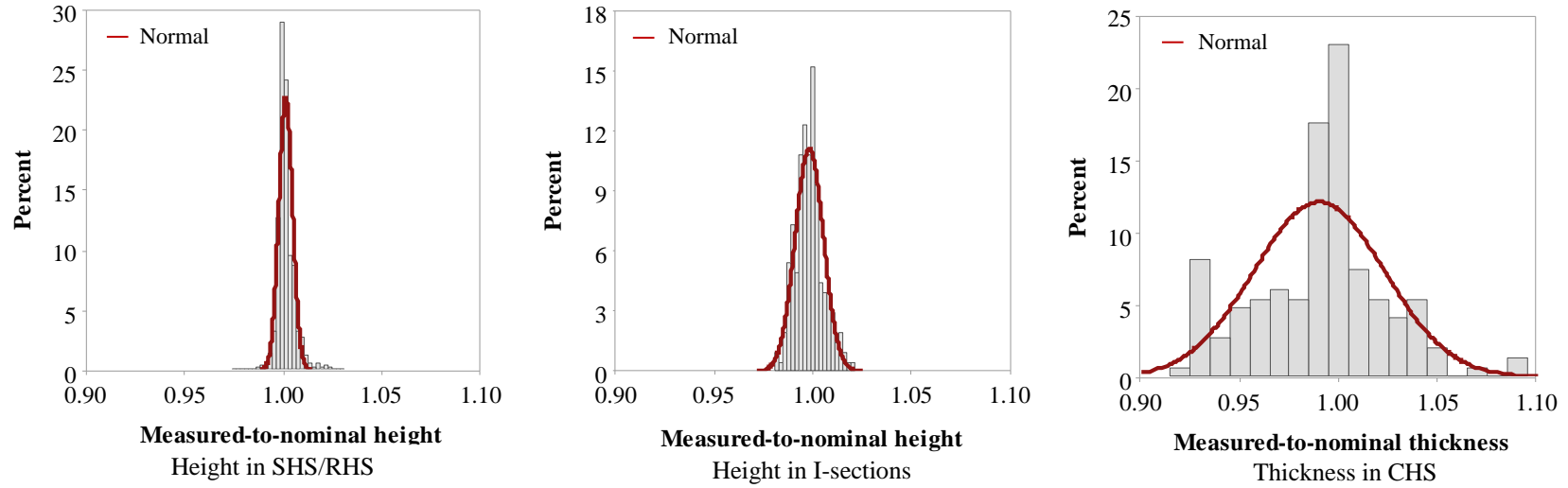


Figure 2. Histograms of cross-section dimensions for different stainless steel section types.

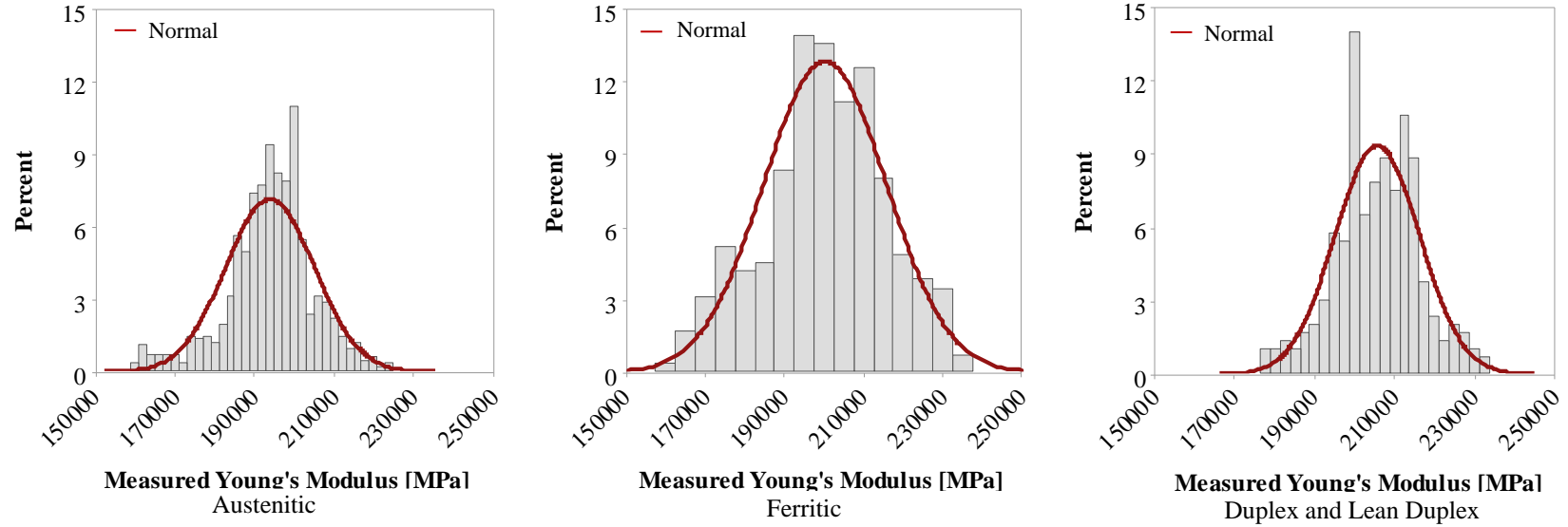


Figure 3. Histograms of Young's modulus E for different stainless steel types.

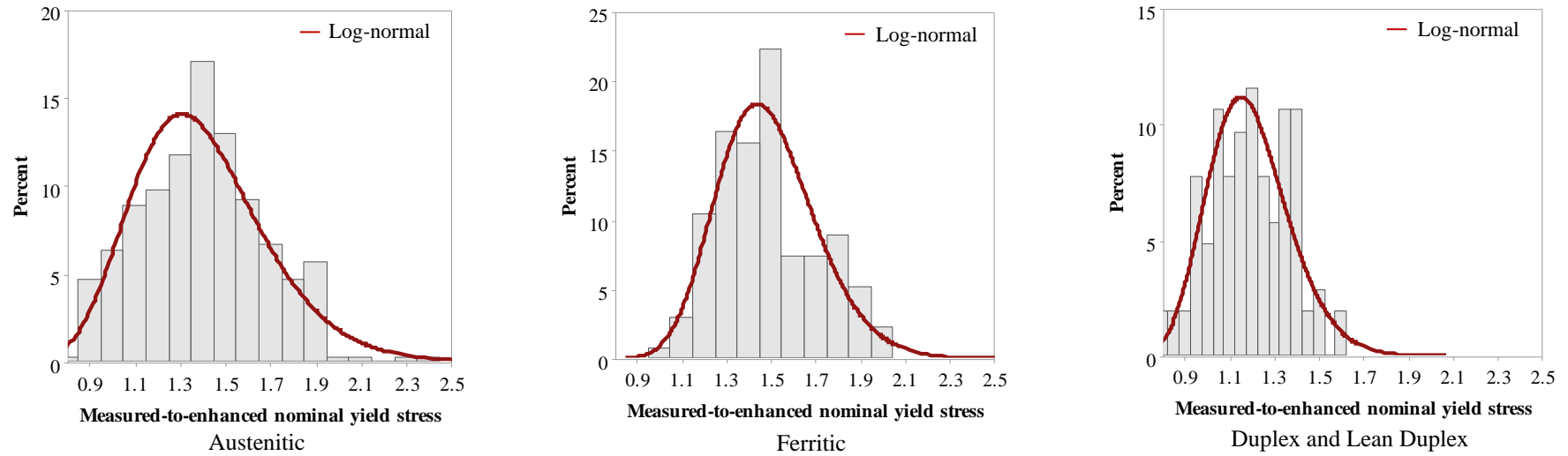


Figure 4. Histograms of yield stress  $f_y$  for different cold-formed stainless steel types.

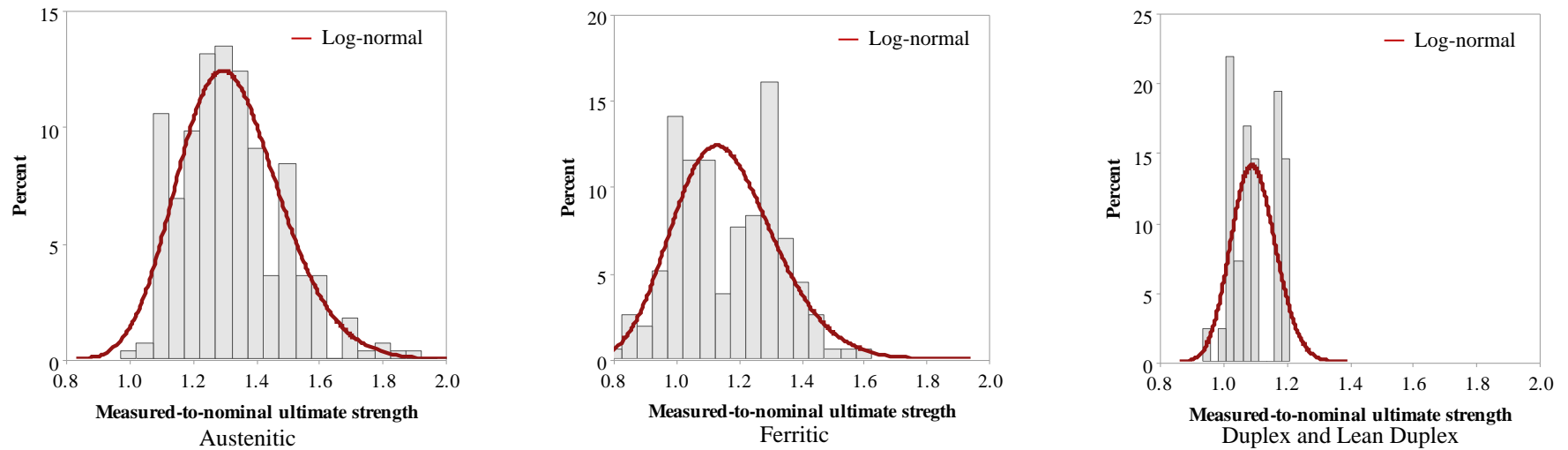


Figure 5. Histograms of ultimate strength  $f_u$  for different cold-formed stainless steel types.

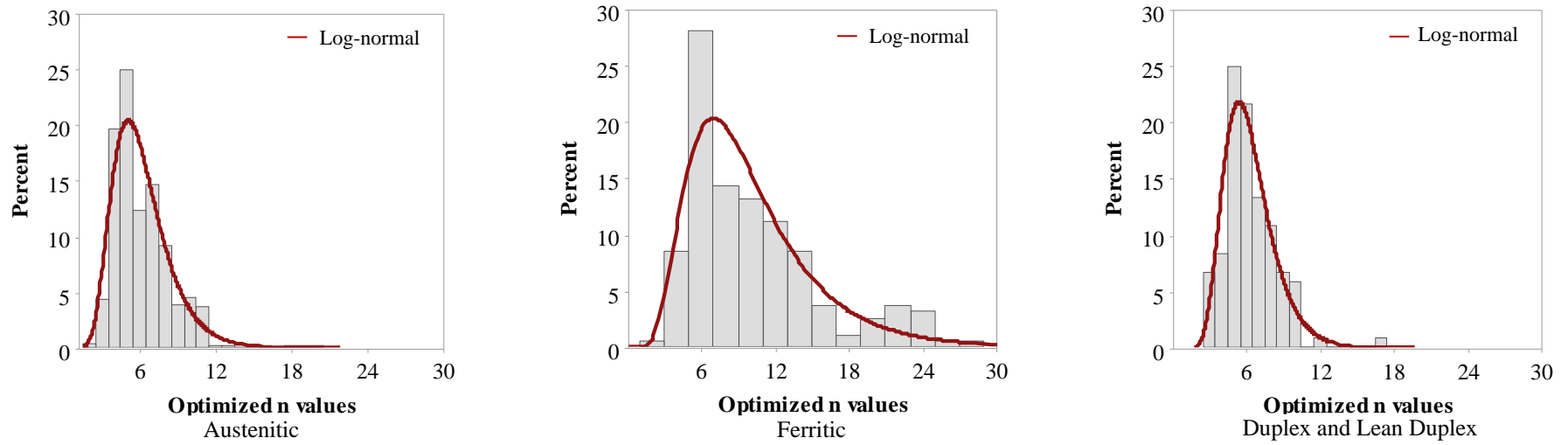


Figure 6. Histograms of strain hardening exponent  $n$  for different cold-formed stainless steel types.

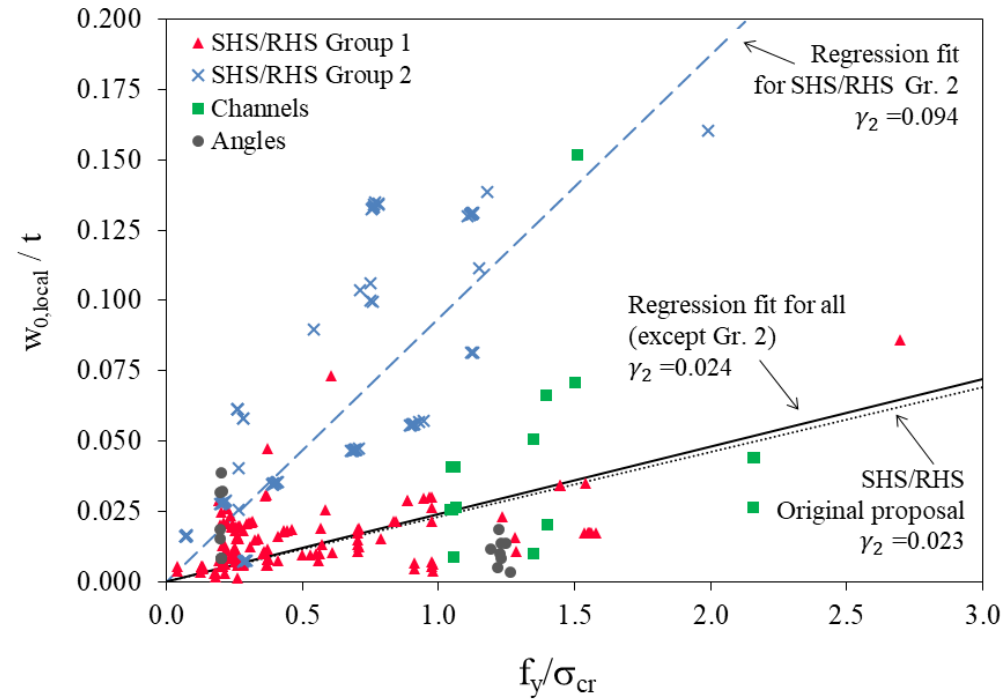


Figure 7. Assessment of predictive models for local imperfection amplitude in stainless steel cold-formed sections.

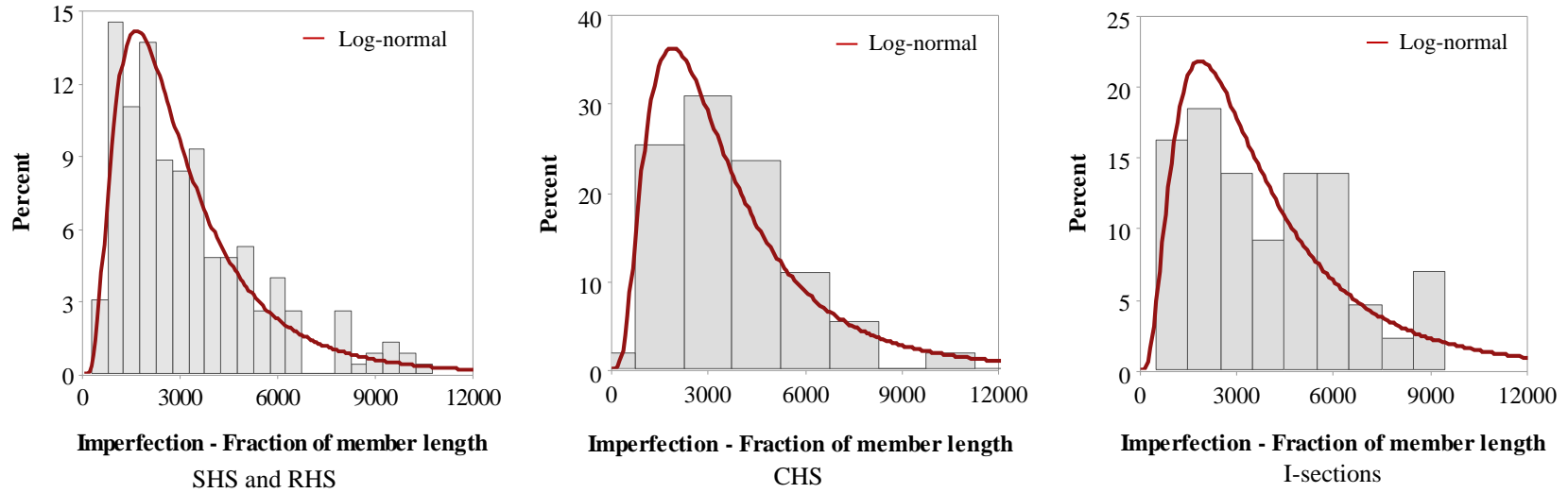


Figure 8. Histograms of member imperfection amplitudes for different stainless steel section types.

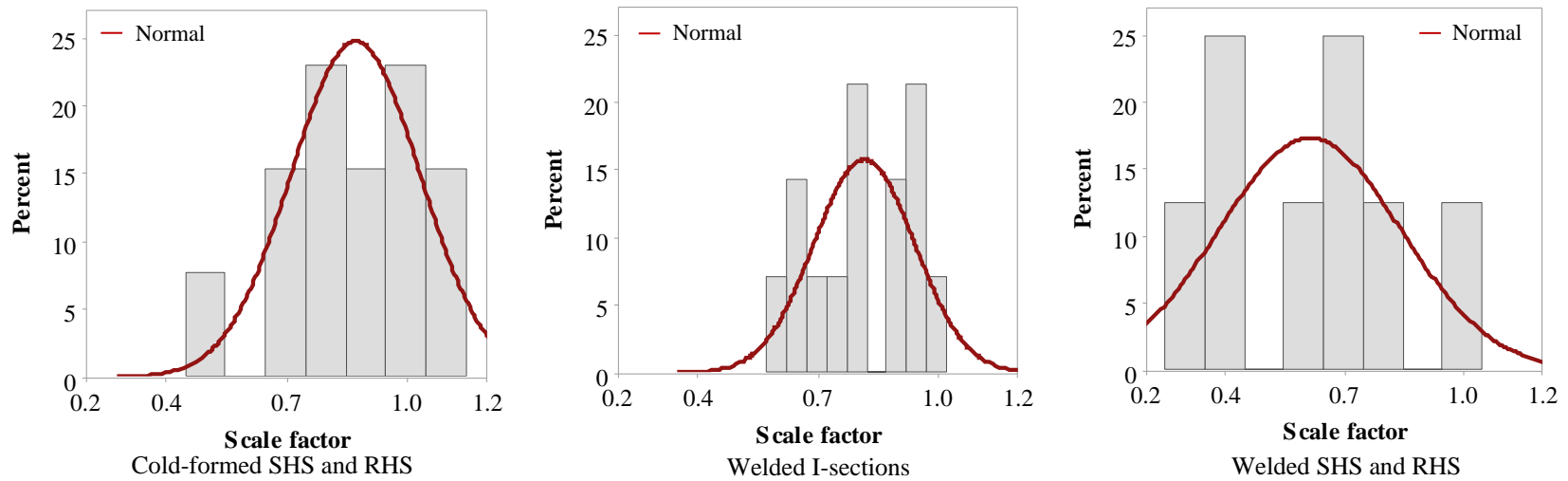


Figure 9. Histograms of residual stress magnitude scale factors for different stainless steel section types.